

AAPM REPORT NO. 87

**DIODE IN VIVO DOSIMETRY
FOR PATIENTS RECEIVING
EXTERNAL BEAM RADIATION THERAPY**

Report of Task Group 62 of the Radiation Therapy Committee

February 2005

Published for the
American Association of Physicists in Medicine
by Medical Physics Publishing

DISCLAIMER: This publication is based on sources and information believed to be reliable, but the AAPM, the editors, and the publisher disclaim any warranty or liability based on or relating to the contents of this publication.

The AAPM does not endorse any products, manufacturers, or suppliers. Nothing in this publication should be interpreted as implying such endorsement.

Further copies of this report (\$15 prepaid) may be obtained from:

Medical Physics Publishing
4513 Vernon Blvd.
Madison, WI 53705-4964
Telephone: 1-800-442-5778 or
608-262-4021
Fax: 608-265-2121
Email: mpp@medicalphysics.org
Web site: www.medicalphysics.org

International Standard Book Number: 1-888340-50-9 (978-1-888340-50-9)
International Standard Serial Number: 0271-7344

© 2005 by American Association of Physicists in Medicine

All rights reserved. No part of this publication may be reproduced, stored in a retrieval system, or transmitted in any form or by any means (electronic, mechanical, photocopying, recording, or otherwise) without the prior written permission of the publisher.

Published by Medical Physics Publishing
for the American Association of Physicists in Medicine
One Physics Ellipse
College Park, MD 20740-3846

Printed in the United States of America

Task Group 62
AAPM Radiation Therapy Committee

Ellen Yorke (Chair), Memorial Sloan-Kettering Cancer Center, New York City, NY
Rodica Alecu, U.S. Oncology, Texas Cancer Center, Sherman, TX
Li Ding, Robert Boissoneault Cancer Institute, Ocala, FL
Doracy Fontenla, Long Island Jewish Medical Center, NY
Andre Kalend, West Virginia University, Morgantown, WV
Darryl Kaurin, Oregon Health & Science University, Portland, OR
Mary Ellen Masterson-McGary, Lutgert Cancer Center, Naples, FL
Ginette Marinello, Hôpital Henri Mondor, Unite de Radiophysique, Créteil, France
Thomas Matzen, Scanditronix Wellhöfer AB, Uppsala, Sweden
Amarjit Saini, H. Lee Moffitt Cancer and Research Institute,
University of South Florida, Tampa, FL
Jie Shi, Sun Nuclear Corporation, Melbourne, FL
William Simon, Sun Nuclear Corporation, Melbourne, FL
Timothy C. Zhu, University of Pennsylvania, Philadelphia, PA
X. Ronald Zhu, University of Texas M.D. Anderson Cancer Center,
Houston, TX

Previous members with input into this report:

Göran Rikner, University Hospital Uppsala, Sweden
Görgen Nilsson, Scanditronix

Acknowledgment: Task Group 62 thanks Mr. James Pinkerton of Sun Nuclear Corporation for his generous editorial assistance.

CONTENTS

Abstract	1
1 INTRODUCTION	1
1.1 Why in vivo dosimetry?	1
1.2 Diodes and this report	3
2 PHYSICS OF THE SILICON DIODE USED AS A RADIATION DETECTOR	3
2.1 Features of diode construction that impact in vivo dosimetry.....	6
2.2 Dependencies resulting from the die	6
2.2.1 Instantaneous dose rate (or dose per pulse) dependence	7
2.2.2 Sensitivity variation with accumulated dose (SVWAD).....	9
2.2.3 Sensitivity variation with temperature (SVWT)	10
2.2.4 P-type versus n-type diode	11
2.3 Dependencies resulting from detector construction	12
2.3.1 Diode shape and directional dependence	12
2.3.2 Energy dependence	13
2.3.3 Field-size dependence	14
2.3.4 Dose perturbation	15
2.3.5 Importance of the buildup.....	15
2.4 Electrometer considerations.....	15
2.4.1 Operational limits	16
2.4.2 Compatibility with diode polarity and sensitivity.....	16
2.4.3 Input offset voltage, series resistance, and diode impedance	17
3 FACTORS TO CONSIDER BEFORE PURCHASING A DIODE IN VIVO DOSIMETRY SYSTEM	18
3.1 Components of a system for measurements at conventional treatment distances	18
3.2 Additional features for TBI measurements	21
3.3 Additional general features	22
4 ACCEPTANCE TESTING	23
5 CALIBRATION	25
5.1 Entrance calibration factor, $F_{cal,en}$	26
5.1.1 Calibration conditions	26
5.1.2 Determining the dose at the DDRP for entrance dosimetry.....	28
5.1.3 Entrance calibration measurements	29
5.2 Exit calibration factor, $F_{cal,ex}$	30
5.2.1 Exit calibration considerations	30
5.2.2 Determining the dose to water at the diode	

	exit-dosimetry reference point	30
5.2.3	Positioning considerations for exit-dosimetry calibration	31
6	CORRECTION FACTORS	31
6.1	Beam-dependent correction factors	33
6.1.1	Entrance SSD correction factor, C_{SSD}	33
6.1.2	Exit dose as a correction factor, $C_{ex,ssid}$	34
6.1.3	Exit SSD correction factors	34
6.1.4	Entrance field-size correction factor, C_{FS}	36
6.1.5	Exit field-size correction factor, $C_{FS,ex}$	37
6.1.6	Entrance accessory correction factor, C_{AC}	37
6.1.7	Accessory correction factors for exit dosimetry	39
6.2	Intrinsic correction factors	39
6.2.1	Temperature correction factor, K_T	40
6.2.2	Angular dependence correction factor, K_θ	41
6.3	Patient dependent correction factors: Thickness, C_{thick} , and gap, C_{gap}	42
7	CONTINUING QUALITY ASSURANCE OF A DIODE IN VIVO DOSIMETRY SYSTEM	44
8	CALCULATING EXPECTED DOSES FOR DIODE IN VIVO DOSIMETRY	46
9	POSITIONING CONSIDERATIONS	48
10	OTHER IN VIVO MEASUREMENT APPLICATIONS OF DIODES AT STANDARD TREATMENT DISTANCES	49
10.1	Out-of-field and skin doses	49
10.2	Intensity-modulated radiation therapy (IMRT)	51
10.3	Kilovoltage therapy	51
11	DIODE IN VIVO DOSIMETRY FOR TOTAL BODY IRRADIATION (TBI)	51
11.1	Rationale for in vivo dosimetry for TBI	51
11.2	Acceptance, calibration, and correction factors for TBI	52
11.2.1	Acceptance measurements	52
11.2.2	Entrance dose calibration	53
11.2.3	Exit dose calibration	54
11.2.4	Correction factors	54
11.3	Phantom measurements to establish action levels	55
11.4	Continuing QA	55
11.5	Comparison of diode readings and expected patient doses	56
11.5.1	Single-point entrance dosimetry	56
11.5.2	In vivo dosimetry to document dose homogeneity	57
12	IN VIVO DIODE DOSIMETRY FOR TOTAL	

ABSTRACT

In vivo dosimetry directly monitors the radiation dose delivered to a patient during radiation therapy. It allows comparison of prescribed and delivered doses and thus provides a level of radiotherapy quality assurance that supplements port films and computational double checks. A well-devised in vivo dosimetry program provides additional safeguards without significantly extending treatment delivery time.

A variety of detectors, including thermoluminescent dosimeters (TLD), silicon diodes, and new detectors such as metal oxide silicon field-effect transistors (MOSFETs) are currently available for in vivo dosimetry. Diodes have gained in popularity since the 1980s because they are rugged, relatively inexpensive, and provide online readings for prompt point-dose inference compared to the offline and lengthy annealing process required with TLD. This real-time in vivo dosimetry allows for immediate investigation and correction of errors encountered during dose delivery.

While many diode systems are marketed as ready plug-and-play for clinical use, medical physics understanding is required for users to accurately and effectively infer delivered doses from diode readings. Task Group 62 (TG-62) was formed to provide physics information, advice, and guidelines to assist clinical physicists in performing reliable in vivo dose verification using diodes. This report provides some basic solid-state physics and electrometer concepts essential to understanding the diode as a dosimeter; describes practical acceptance tests, calibration, and correction methods for commissioning a diode in vivo dosimetry system; and suggests methods of inferring doses to patients undergoing static photon and electron beam radiation therapy. It also discusses considerations that can assist physicists in making new purchases or in implementing a clinical diode in vivo dosimetry program.

1 INTRODUCTION

1.1 Why in vivo dosimetry?

In vivo dosimetry is the most direct method for monitoring the dose delivered to the patient receiving radiation therapy. When performed early in treatment as a supplement to the clinical quality assurance (QA) program, simple in vivo measurements are an additional safeguard against major setup errors and calculation or transcription errors that were missed during pre-treatment chart check.^{1,2,3,4,5,6,7} In the absence of errors, routine in vivo measurements uniquely document that treatment was delivered correctly within a user-specified tolerance. Unlike other QA methods, in vivo dosimetry checks the dose delivered to the patient rather than the individual components prior to treatment. Most treatments are without serious error—in a recent review from Europe, out of 10,300

patients at three institutions performing in vivo dosimetry for all new patients, 120 treatment errors exceeding 5% were found, and the estimated serious error (misadministration) rate in the United States is 0.002%.⁸ Although there is not universal agreement on the benefit of in vivo dosimetry,⁸ a strong argument in its favor is that preventing the severe consequences of major errors—as illustrated by the recent overexposure of 28 patients in Panama—warrant the effort and expense of an in vivo dosimetry program.^{9,10,11} In vivo dosimetry is also helpful in supporting the high accuracy in dose delivery expected from complex and conformal therapy techniques.⁴ For these and other reasons, AAPM TG-40 recommends that clinics “should have access to TLD or other in vivo systems.”¹²

Most in vivo dosimetry employs either silicon diodes or thermoluminescent dosimeters (TLDs). TLD dosimetry has been used for over 30 years. It is the method of choice in many large departments, and the subject of much literature.^{1,13,14} However, diodes have gained popularity since the early 1980s due to their rapid processing time (seconds vs. hours for TLD) and high sensitivity (over 18,000 times that of an air-filled ionization chamber of the same volume).^{14,15,16,17} With care, diodes may equal or even surpass the accuracy of TLD¹⁸ for in-field measurements.

TLD and diodes are used similarly for external beam in vivo measurements, although the underlying physics is very different. The dosimeter is placed on the patient’s skin, and the dose to a point of interest inside the patient is inferred from surface measurements. In vivo entrance measurements, where dose at a point within the patient is inferred from the reading of a detector on the entrance surface and compared with calculation, can detect numerous serious errors including an incorrect daily dose, treatment with the wrong beam energy, omission or use of the wrong wedge, and setup errors such as a patient set up with SAD (source-to-axis distance) rather than SSD (source-to-phantom surface distance) technique.^{1,19,20} Changes in treatment machine output between calibrations have also been reported.^{1,4} Combined in vivo measurements at both entrance and exit points, while introducing extra complexity,²¹ can detect additional errors, including large errors in patient thickness and problems with the dose calculation algorithm or data in the planning system.^{1,4,7,21} For total body irradiation (TBI), combined entrance and exit measurements are used to assess the adequacy of missing tissue compensation.^{22,23}

The ranges of discrepancy between expectation and measurement beyond which clinical action must be taken are referred to as action or tolerance levels—below, we shall call these simply “action levels.” Regardless of the dosimeter used in an in vivo dosimetry program, the size of action levels and the associated actions are key decisions, requiring careful consideration of the clinical goals of the program and the accuracy that is reasonably achievable with the available personnel and equipment. An interesting review of the “philosophies and results” of in vivo dosimetry has recently been published.¹

1.2 Diodes and this report

Even off-the-shelf diode systems purchased from reputable vendors require care, skill, and understanding on the part of their users for accurate in vivo dosimetry. Task Group 62 (TG-62) was formed to provide guidelines for clinical physicists performing in vivo diode dosimetry. This report deals with applications to external beam, static-field treatments—the area in which there is enough clinical experience to provide reliable information.

In vivo dosimetry is supplementary, not mandatory, to a good clinical QA program.^{8,12} Thus the aim of this report is to provide guidance and information, rather than rules. Section 2 reviews the physics of silicon diodes to provide understanding of the basis for the cautions, calibrations and corrections discussed in the subsequent sections. Sections 3 and 4 are directed to users who are purchasing a new diode system. Section 5 deals with diode calibration and Section 6 with correction factors that may be required to handle a wide range of treatment field geometries. Section 7 deals with continuing QA of the system. Anticipating that some readers may move directly to the practical matters of sections 3 through 7, these sections include references back to the physics review in section 2. Section 8 briefly discusses methods for comparing diode readings with calculated doses, and section 9 deals with important clinical issues of diode positioning for in vivo dosimetry. Section 10 briefly describes other in vivo uses of diodes at standard distances that are of potential interest but are not yet well documented. Sections 11 and 12 discuss the use of diodes for total body irradiation (TBI) and total skin electron therapy (TSET), respectively. Finally, section 13 is a beginner's guide to establishing a diode in vivo dosimetry program. A report on diode dosimetry, including an extensive review of the European experience, has recently been published by ESTRO (European Society of Therapeutic Radiology and Oncology).²⁴ The TG-62 report is complementary to the ESTRO document in that it places more emphasis on the U.S. experience and provides an extensive review of the physics of diode dosimetry and guidance for the use of diodes for TBI and TSET.

2 PHYSICS OF THE SILICON DIODE USED AS A RADIATION DETECTOR

For over 30 years, the silicon semiconductor diode has been used as a radiation detector.^{25,26,27,28} The density of silicon and the low average energy required to form a carrier pair in silicon results in a radiation current density which is about 18,000 times that of air, allowing a small volume (approximately $10^{-2} \sim 10^{-1} \text{ mm}^3$) of silicon diode to produce an easily measured current. As a result, diodes have a high sensitivity (defined as charge collected per unit dose to the diode). Their small volumes, mechanical ruggedness, and real-time readout make diodes attractive for in vivo dosimetry. However, the physics of charge

generation and collection in semiconductor diodes introduces characteristic features that are relevant to their accurate clinical use in this application.

The key structure in the silicon diodes used for in vivo dosimetry is the pn junction. N-type silicon is doped with impurities of a pentavalent element (e.g., phosphorous) called a “donor.” Each donor can contribute a free electron to the silicon. Therefore, the majority carriers in n-type silicon are electrons, and holes are the minority carriers. P-type silicon is doped with impurities of a trivalent element (e.g., boron) called an “acceptor.” Each acceptor can accept an electron, resulting in a mobile hole in silicon that is equivalent to a positively charged carrier. In p-type silicon, holes are the majority carriers while electrons are the minority carriers.

Both n-type and p-type diodes are commercially available. An n-type diode is formed by doping acceptor impurities into a region of n-type silicon. A p-type diode is formed by doping donor impurities into a p-type substrate. In either case, a spatially varying doping creates a region where p- and n-type silicon are in direct contact. The majority carriers from each side diffuse to the opposite side, i.e., electrons on the n side diffuse to the p side, leaving positively charged donor ions behind, while holes on the p side diffuse to the n side leaving behind negatively charged acceptor ions. These oppositely charged ions establish an electric field (the “built-in potential”) that, at equilibrium, prevents further diffusion of the majority carriers. This spatially charged region is the pn junction, also called the “depletion region.” For diodes used for in vivo dosimetry, the typical width of the depletion region is less than several microns. Although the typical built-in potential is less than 1 volt, the electric field across the pn junction is very high (greater than 10^3 V/cm). If the diode were connected to an idealized, leakage-free electrometer, no current would flow unless excess carriers were injected by external sources, such as bias voltage, light, heat, or ionizing radiation.

Charge collection in a semiconductor diode is very different than in an ionization chamber. While an ionization chamber requires a high voltage supply, the high electric field across the pn junction makes charge collection possible for the diode without external bias. As schematically illustrated in figure 1, the incident ionizing radiation generates electron-hole pairs throughout the diode. The minority carriers (electrons on the p side and holes on the n side) diffuse toward the pn junction. Those carriers within approximately one diffusion length from the junction edge are able to reach it before they recombine. They are then swept across the junction by the built-in potential and measured by the electrometer. The total current consists of the radiation-induced photocurrent (below, called “radiation current”) and the electrical leakage current due to the offset voltage from the electrometer.

The processes that determine how many of the mobile charges generated by radiation are collected are also very different from those in an ionization chamber. Direct recombination, which dominates in an ionization chamber, is

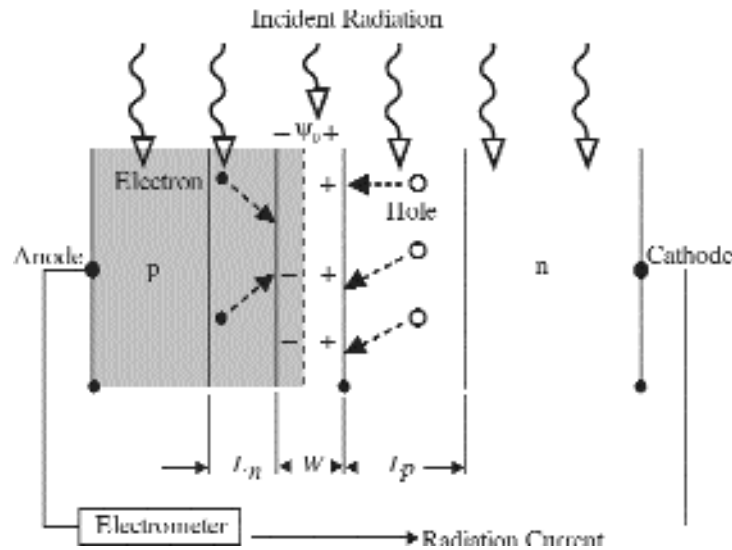


Figure 1. Schematics of a Si pn junction diode as a radiation detector. The excess minority carriers (electron—• and hole—o) generated by radiation within one diffusion length, L_p on the n side and L_n on the p side (lightly shaded region), are able to diffuse to the pn junction (width W). They are then swept across the junction by the built-in potential ψ_0 and are collected by the electrometer.

highly improbable in silicon. The dominant mode in a silicon diode is indirect recombination. This is a function of material defects, which facilitate recombination, and also of the density of radiation-generated electrons and holes. Indirect recombination determines the lifetime of radiation-generated carriers and thus the fraction of carriers that diffuse to the pn junction and are collected. Thus, the carrier lifetime controls the diode sensitivity (the charge collected per unit dose to the diode). Exposure to large ($>kGy$) doses from a high-energy beam (>2 MeV) produces radiation-damage defects which shorten the minority carrier's lifetime and reduce the diode's sensitivity. Indirect recombination is responsible for a sensitivity change with instantaneous dose rate (for linear accelerators, dose per pulse), which is a major cause of the variation of the diode sensitivity with SSD. The magnitude of these sensitivity changes depends upon the material characteristics of the diode (e.g., n- or p-type, doping levels (resistivity), and pre-damage of the material). See reference 29 for additional general information about pn junction diodes, reference 30 for indirect recombination, and reference 31 for an overview of the interplay between material properties and the sensitivity of clinical diodes.

2.1 Features of diode construction that impact in vivo dosimetry

A diode is a two-terminal device, meaning there are two electrodes that require connection (see figure 1). Coaxial cables and connectors are used in the assembly of diode detectors. This is an important difference from a guarded ionization chamber, which is a three-terminal device and requires a triaxial cable and connector. Most electrometers used with ionization chambers have triaxial input and cannot be transferred to diodes without an appropriate triaxial-to-coaxial adapter.

The two terminals of the diode can be connected to the coaxial cable in two different configurations that result in either a positive or negative signal from the diode detector. A negative diode detector is made by connecting the center conductor of the cable to the cathode of the diode, while a positive diode detector connects the center conductor to the anode of the diode (see figure 1). This choice does not affect the performance of the detector and is made by the manufacturer to match the input polarity requirement of the electrometer.

The silicon piece in the diode that was described above is commonly referred to as the “die.” The dimensions and shape of the die are similar to those of a TLD chip. The construction of the die, including size, composition of the doping, the forming of the pn junction by diffusion, and any lattice defects, either initially present or caused by irradiation, determine some of the characteristics of the detector response to radiation.

For in vivo dosimetry, the die is covered with material both for protection and to provide buildup material. Electron in vivo dosimetry diodes have minimal buildup ($\leq 0.3 \text{ g/cm}^2$) but are otherwise the same as photon diodes. The commercial diode detector, commonly called “the diode,” is the complete assembly including the die, its attached terminals, a protective cover, and buildup material.

Figure 2 shows the external appearance of three common types of photon diodes and one electron diode. Figure 3 shows schematic diagrams of these same devices. The overall construction determines many of the diode radiation response characteristics, including response dependence on beam direction, energy, field size, and aspects of the SSD dependence.

Finally, the diode is operated together with an electrometer. The electrometer input specifications, such as series impedance, input offset voltage, and amplifier polarity may affect measured results. The next three subsections outline how these systems affect the response of a diode to ionizing radiation.

2.2 Dependencies resulting from the die

The radiation-induced current and the diode sensitivity are proportional to the diffusion length of the minority carrier, which, in turn, is proportional to the square root of the product of the carrier diffusion coefficient (which is proportional to the carrier mobility) and the carrier lifetime. The carrier lifetime is

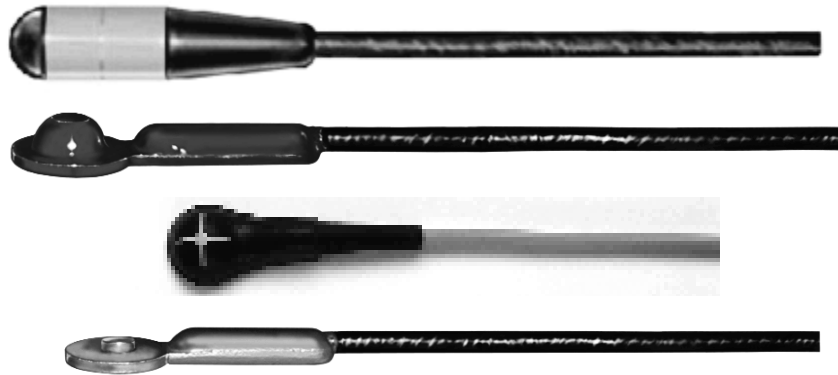


Figure 2. Typical diodes used for in vivo dosimetry.

the dominant factor determining several important characteristics of the diode sensitivity in the context of in vivo dosimetry. These include:

1. The instantaneous dose-rate dependence of the sensitivity, which is responsible for much of the change in diode response with its distance from the radiation source (commonly called “SSD dependence”) and with beam modifiers such as wedges.
2. The decrease in sensitivity with accumulated dose.
3. The temperature dependence (or temperature coefficient) of diode sensitivity. The temperature coefficient also depends on the diffusion coefficient.

2.2.1 Instantaneous dose rate (or dose per pulse) dependence^{30,31,32,33}

There are always defects and impurities in a semiconductor crystal that introduce RG (recombination-generation) centers. Indirect recombination, which occurs when a minority carrier is captured by an RG center and then recombines with a majority carrier, is the dominant process of charge recombination in a silicon diode. The fraction of minority carriers which recombine depends on the concentration of RG centers, on their capture cross sections for the minority carriers, and on the excess carrier concentration, which is proportional to the instantaneous dose rate. During a single radiation exposure typical of a radiation therapy treatment (<10 Gy) the population of RG centers remains approximately constant. When the instantaneous dose-rate increases (e.g., due to treating at a short SSD), the rate of minority carrier generation also increases. If the RG center concentration is insufficient to keep the recombining fraction of carriers constant, the diode sensitivity increases because a larger fraction of the charge produced by the radiation is available to be collected by the electrometer. This effect is counter-intuitive from the perspective of ionization chambers. For linacs, dose is delivered in pulses (~100 pulses per second of width ~2 to 6 μ s) and the instantaneous dose rate within a single radiation

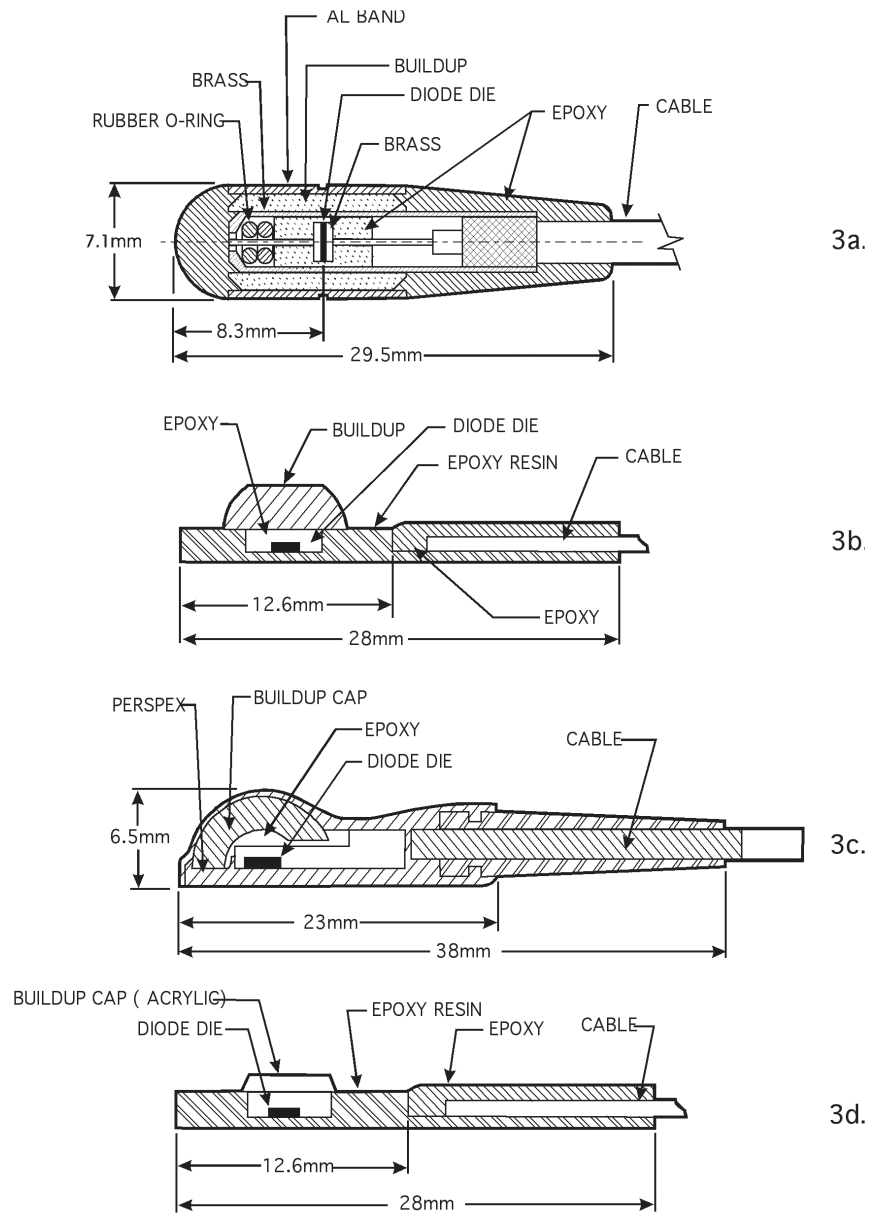


Figure 3. Typical diode construction showing the major components and internal arrangement of the diodes in Figure 2. (3a: cylindrical Sun Nuclear photon diode; 3b: flat/hemispherical Sun Nuclear photon diode; 3c: flat/hemispherical Scanditronix Wellhöfer diode; 3d: Sun Nuclear electron diode.)

pulse determines the rate of charge generation. Therefore, the instantaneous dose-rate effect is often called the “dose per pulse dependence” (dose per pulse is the product of the pulse width and the instantaneous dose rate).

All diode detectors exhibit some change in sensitivity with SSD and with the presence of beam modifiers such as wedges. This is partly because changes in SSD or beam attenuation change the instantaneous dose rate at the die and thus change the probability of indirect recombination. The magnitude of instantaneous dose rate dependence is determined by the characteristics of the die and the dominant RG center.

It is important, however, to realize that scattered radiation, especially electron contamination, may also contribute to the SSD dependence of the diode sensitivity, causing sensitivity changes to depend upon the buildup thickness.^{34,35,36,37} Pure dose per pulse dependence of diode sensitivity is difficult to measure in isolation from the effects of scattered radiation.

It is also important to note that the average dose rate (nominally 100 to 600 cGy/min) that is set at the accelerator console is not the same as the instantaneous dose rate in an accelerator pulse (10^3 to 10^4 cGy/sec). The dose rate in the pulse is 10^2 to 10^3 times higher than the average rate. Because the charge collection time of the diode and electrometer is typically much shorter than the time between pulses, the response of an in vivo dosimetry system is not expected to depend upon average dose rate. However, the average dose-rate dependence of the system should be evaluated when the system is commissioned as it might identify electrometer problems (see section 2.2.4).

2.2.2 Sensitivity variation with accumulated dose (SVWAD)^{15,31,32,33,38}

Any mechanism that causes crystal damage introduces defects in a silicon diode. These mechanisms, which include intentional doping with impurities such as platinum and gold and also ionizing radiation, result in a sensitivity variation with accumulated dose (SVWAD). The defects produce RG centers and carrier traps (defects which capture carriers but have a very small probability for recombination), both of which reduce the diode sensitivity.

The radiation damage in therapy photon beams stems from the recoil energy of secondary electrons and in electron beams from the energy of primary and scattered electrons that is imparted to the silicon crystal lattice. Accumulated dose increases the number of RG centers, causing a reduction in carrier lifetimes and a consequent decrease in diode sensitivity and changes in SSD dependence. The damage coefficient expresses the dependence of diode sensitivity degradation on the energy of the irradiating beam.³⁹ For electron energies below about 0.7 MeV, the damage coefficient is low. Therefore, the SVWAD is small for photon or electron beams with energies below approximately 1 MeV (Co-60). The damage coefficient increases rapidly between 0.7 and 2 MeV and plateaus above 2 MeV.³⁹ Clinical electron beams are more damaging per unit dose accumulated than photon beams because clinical electron beam energies are above the plateau. It is also found that high-energy photon beams (>10 MV)

cause greater damage to silicon diodes than expected from the average recoil energy of the electrons. This may be due to the neutron contamination. Although the percentage of the neutrons in a photon beam is low, their damage coefficient is much higher.⁴⁰

The rate of SVWAD is reduced by an increase in the defect density. Therefore, manufacturers often pre-irradiate diodes with electron beams or use platinum doped silicon to deliberately increase the defect density. While these techniques reduce the initial sensitivity of the diode, its performance then changes less with clinical use. Vendors should provide an estimate of the SVWAD in a specified beam quality. For diodes currently marketed by several vendors, the quoted decrease ranges from <0.1%/kGy in a 6 MV photon beam to 16% /kGy for a low buildup diode in a 21 MV photon beam.

Because vendors quote generic values of SVWAD, diode sensitivity and SSD dependence should be measured periodically as part of the clinical QA process. A recent study reports a sensitivity decrease of 3.4% per 100 Gy for one variety of diode and 0.2% per 100 Gy for a second variety, both irradiated with an 18 MV photon beam.³⁷ Another recent study⁴ reports an average sensitivity decrease of 0.7% per kGy for diodes used in 4, 6, and 8 MV beams.

2.2.3 Sensitivity variation with temperature (SVWT)

The radiation current generated in a diode may either increase or decrease with increasing temperature,²⁸ resulting in a diode sensitivity variation with temperature (SVWT). The “temperature coefficient” is the percent change in sensitivity per degree of temperature increase. Modeling the temperature dependence from first principles is very difficult as it is determined by the temperature dependence of carrier mobility and lifetime, which may have opposite variation trends.³³ The carrier mobility generally decreases as temperature increases due to higher crystal lattice scatter.^{28,30} The carrier lifetime appears to increase with increasing temperature due to the increased probability of carrier release from the RG centers and traps. Most diodes used for in vivo dosimetry have a positive temperature coefficient (i.e., sensitivity increases with increasing temperature). The SVWT tends to first increase with large (>kGy) accumulated dose and then stabilize with further dose,^{32,41,42,43} probably due to the generation of additional RG centers and traps so that more carriers are released as the temperature increases. For these diodes, the dependence of carrier lifetime on temperature is the dominant effect. The change in sensitivity of commercial diodes used for in vivo dosimetry is typically between +0.1 and +0.54%/°C.^{37,42,43,44}

A user should check product specifications for estimates of typical temperature coefficients or SVWT and to determine whether automatic temperature compensation using the diode itself as a thermistor is available.^{32,44,45} Steps to reduce or correct for effects of SVWT on in vivo measurements are discussed in sections 5.1.3 and 6.2.1. Regardless of whether the user chooses to correct

for temperature dependence, it is important to be aware of how it affects in vivo measurements.^{43,45}

The diode leakage current has a much higher temperature coefficient than the radiation-induced current (as high as +15%/°C). Although the leakage current is usually much smaller than the radiation current at room temperature^{29,33,46}, leakage could contribute a significant portion to the observed temperature dependence of the diode response, especially for diodes with low impedance and electrometers with high offset voltage.

2.2.4 P-type versus n-type diode

Some literature reports that p-type diodes are better than n-type diodes in terms of SVWAD and dose per pulse dependence.^{15,32,33,40,47} The theory behind this is that the radiation-generated RG centers have a larger capture cross section for holes than for electrons. Therefore, during radiation exposure, more RG centers are occupied by the minority carriers (holes) in an n-type than in a p-type diode (where the minority carriers are electrons). The same change in excess minority carrier concentration produces a greater reduction in the population of unoccupied RG centers in an n-type than in a p-type diode, making for more charge collection and a larger increase in sensitivity with dose rate in an n-type than in a p-type diode.

However, this theory assumes that the RG centers generated by electron pre-irradiation are the dominant ones, and that all device parameters in the n- and p-type diodes are the same (substrate resistivity, junction size, the probability of creating a RG center under radiation, etc.). In reality, these conditions may not apply because diode detectors differ from each other in the following aspects:

1. Lower substrate resistivity (higher concentration of the majority carrier) increases the probability of indirect recombination with the minority carriers and thus results in lower dose per pulse dependence.^{31,33,41}
2. There are always initial defects and impurities introduced during the formation of a pn junction which also serve as RG centers. These may have quite different capture cross sections for minority carriers than the RG centers generated by electron pre-irradiation. They can also affect the probability of creating radiation-induced RG centers. Thus, the initial defects can make a diode either better or worse relative to its performance with or without pre-irradiation.^{15,31,32,33,40,42,47}
3. The level of pre-irradiation or platinum doping affects carrier lifetime, sensitivity degradation rate, and dose per pulse dependence.^{31,33,38,40,42}

Furthermore, a diode detector with inadequate buildup could have significantly larger SSD dependence due to the dose from contaminant electrons in combination with its intrinsic dose per pulse dependence.^{36,37}

Complex interplay between these factors, rather than a simple “n vs. p” distinction determines the SVWAD and the SSD dependence of a particular diode.

Therefore, the user is advised to evaluate the available information from vendors and current publications rather than to generalize that p-type diode detectors are always superior to n-type detectors.

2.3 Dependencies resulting from detector construction

2.3.1 Diode shape and directional dependence^{34,46,48}

The reading per monitor unit (MU) of a diode placed on a patient's skin or phantom surface depends on its orientation with respect to the incident direction of the beam. This directional response is caused partly by the detector construction (including transmission through varying thicknesses of the buildup or cable at large angles) and partly by back scattering from the patient or phantom. Vendors typically state estimates of the change in effective sensitivity (diode reading per MU) with beam direction and should specify the conditions under which these estimates apply.

Two general methods of construction for diode detectors define the symmetry of the directional response. Each type has advantages in some clinical situations. Figures 2 and 3 show the external appearance and schematic diagrams for example diodes of both types, and figure 4 shows the principle directions that describe the angular dependence.

1. Figures 2(a) and 3(a) have cylindrical symmetry. The plane of the die is mounted normal to the cable axis and the die is surrounded with a cylindrical sleeve of buildup [figure 3(a)]. For in vivo dosimetry, the side of the cylinder should be against the patient with the beam axis as nearly normal to the cylinder axis as possible so the plane of the die is approximately parallel to the beam axis. Cylindrical detectors have relatively small directional dependence when the beam axis rotates in the axial direction [figure 4(a)], with effective sensitivity changing by <2% for angles less than $\pm 70^\circ$. The major directional dependence is determined by the "tilt" angle between the beam axis and the axis of the cylindrical detector, as shown in figure 4(b). Therefore, it is better to use carefully positioned cylindrical diodes for oblique photon beams such as breast tangents.
2. The diodes in figures 2 and 3(b-d) have conical or hemispherical symmetry. The die is mounted with the plane of the die parallel to the cable axis. One side of the die is covered with an approximately hemispherical buildup while the other side has a thin, flat, mainly protective covering. The detector is designed to be placed with the flat side on the patient and the central axis of the beam approximately normal to the plane of the die. The major directional dependence is specified in terms of the angle between the beam axis and the line normal to the die (i.e. to the flat side of the detector), as shown in figure 4(c). These detectors have a relatively strong directional

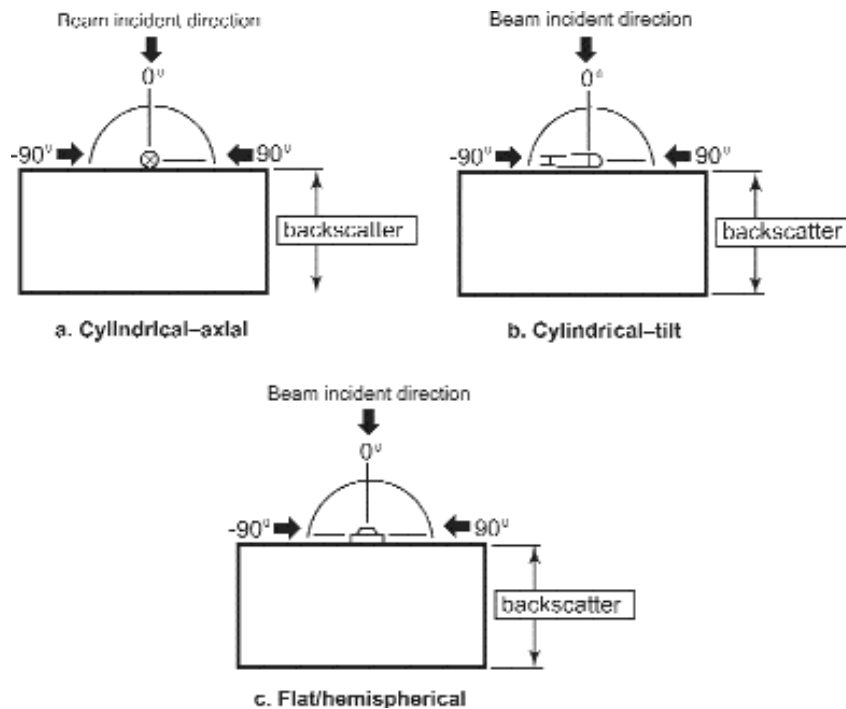


Figure 4. Angular dependences of cylindrical and flat/hemispherical diodes. For optimal placement of a cylindrical diode, the diode axis (a) should be perpendicular to the beam with zero tilt angle (b). For optimal placement of a flat/hemispherical diode (c), the plane of the diode should be perpendicular to the beam axis.

dependence, which can exceed 5% for beam angles exceeding $\pm 40^\circ$. When using such detectors for exit dose measurements, the flat side (no buildup) should be placed against the phantom or patient surface.

The directional dependence of an electron diode could be quite different from that of a photon diode, especially at large angles.⁴⁹ The length of the cone restricts achievable gantry angles for flat phantoms and special measures, such as placing the diode on plastic wedges on a cylindrical phantom^{48,49} have been used to more thoroughly investigate the directional dependence of electron diodes in isolation from phantom effects.

2.3.2 Energy dependence^{36,50,51,52}

The radiation-induced charge per MU in diodes designed for in vivo dosimetry often depends on beam energy. Although the mass absorption coefficient

and the stopping power of the silicon die contributes to the energy dependence for photon and electron beams respectively, most of this energy dependence is due to the materials around the die, such as the electrode attachment, protective housing, and buildup. It is not uncommon to have combinations of Al, Cu, Sn, Au, Ag, Pb, W, Ta, and Fe surrounding the die. Some diodes use foundry products that may already have a high Z electrode attached to the die, while other detectors are manufactured from the bare die with wire bonding techniques that minimize the electrode materials. Scattered electrons from these high Z materials in close proximity to the die contribute to the ionization in the die in amounts that depend on construction details of the diode model.

For photon beam in vivo dosimetry, vendors provide different detectors dedicated to different energy ranges. Both the composition and thickness of the buildup for these diodes are designed with consideration of the depth of the buildup region for the energy range of interest (d_{\max}) as well as of directional dependence and physical size. A diode designed for optimal use at 6 to 12 MV might have a higher response per MU to 18 MV photons due to dose from contaminant electrons which are not stopped by the buildup. Contaminant electrons might also cause a 6 to 12 MV detector to exhibit a strong SSD and field-size dependence if used in an 18 MV beam.²¹ On the other hand, the attenuation of a detector designed for 15 to 25 MV photons reduces its effective sensitivity in a 6 MV beam. The difference could be greater if a higher Z buildup material such as W or Ta is used for the 15 to 25 MV detector.

For electron in vivo dosimetry, a single diode model with minimal buildup generally covers the entire clinical energy range. The energy dependence of the diode response per MU results mostly from the energy dependence of the electron depth dose curve, due to which the sensitive volume of the diode is at different percent doses for different beam energies.⁴⁸

2.3.3 Field-size dependence

For photon entrance in vivo dosimetry, the diode reading per MU increases with increasing field size. For large (40×40 cm²) fields, the diode field-size dependence can differ by up to 5% from the ion-chamber measurements of field-size dependence that are summarized as the total scatter factor ($S_{c,p}$).^{16,22,34,48,53,58} The diode field-size dependence is observed to vary among different commercial diode detectors. For diodes with insufficiently thick buildup, electron contamination is a contributing factor.¹⁴ Additionally, for $S_{c,p}$ measurements, the ion chamber is inside the phantom, while for diode field-size dependence measurements, the diode is on the surface. Thus, the two dosimeters receive different scattered photon contributions.⁵⁴ The diode field-size dependence for exit dosimetry is not necessarily the same as for entrance dosimetry (see sections 6.14 and 6.15).

2.3.4 Dose perturbation^{16,48,55,56,57}

When a diode is used for entrance dose determination, there is a decrease in dose (a dose shadow) below the diode which depends on the effective thickness of the diode, beam modality and energy, field size, and the depth of interest.

For fractionated photon treatments, if in vivo dosimetry is performed once a week or only at the first treatment, this is seldom a clinical problem. For example, measuring once or twice over a course of 20 to 40 treatments has negligible effect as the area of the shadow is small ($<2 \text{ cm}^2$)⁵⁹ and even a 10% “cold spot” in one fraction out of a total of 30 has less than 0.5% effect. Nonetheless, partly to reduce the dose shadow, vendors offer photon detectors designed for several energy ranges. Those designed for the highest energies have the most buildup. Within its designated range, a detector’s dose shadow (10×10 field, 4 to 5 cm depth) should not exceed 5% to 6%, but if it is used for lower-energy photon beams, the perturbation can exceed 10%.

Diodes designed for electron in vivo dosimetry have thin buildup (0.1 to 0.35 g/cm²), but the combined thickness of the non-tissue-equivalent die, leads, and protective housing can produce a dose shadow exceeding 20% at d_{max} for 6 and 9 MeV electrons.^{49,55}

2.3.5 Importance of the buildup

It can be seen from the previous sections that the buildup of a diode detector strongly affects its response to radiation conditions. To reduce the need for corrections in clinical use, it is preferable to use a diode detector within the energy range for which it was designed. Using a low-energy detector for high-energy beams is especially problematic, as it accentuates the effects of contaminant electrons. Use of a high-energy photon detector in low-energy photon beams causes deeper dose shadows. Whether this is a matter of concern depends on the fraction of treatments at which in vivo measurements are performed. However, use of a photon diode for an electron beam produces a particularly deep dose shadow and should be avoided.

If a photon diode is used for in vivo dosimetry outside its specified energy range or for more than one energy, calibration and measurement and assessment of all correction factors should be performed for each beam energy of clinical use. Particular caution is advised if the total buildup thickness is significantly smaller than d_{max} for the photon energy range in which it will be used.^{36,37,60}

2.4 Electrometer considerations

Two basic types of signal conversion are used in electrometers: charge-to-pulse converter (CPC) and analog-to-digital converter (ADC). Both determine accumulated dose by measuring the charge accumulation on the feedback capacitor of the input amplifier. The specifications of the electrometer and detectors should be reviewed together in order to assure proper operation for in vivo measurements.

2.4.1 Operational limits

2.4.1.1 CPC electrometers

A CPC electrometer counts the number of precision charge pulses required to maintain the feedback capacitor at zero net charge during the measurement. In such a circuit, the charge from the diode is collected on the feedback capacitor. As the charge accumulates, the voltage output of the op-amp increases to a level that causes a circuit comparator to initiate a pulse of charge to flow back to the input. This charge pulse defines the resolution of the measurement. The charge-pulse frequency defines the maximum average current that can be measured without causing the voltage across the feedback capacitor to exceed the op-amp supply voltage. To test that the electrometer current limit is not being exceeded in clinical use, compare the diode response per unit dose at the maximum and minimum average linac dose rate (MU/minute). If the diode response per MU at the maximum rate is lower than at the minimum rate, then the electrometer current limit is exceeded.

Radiation produced by linear accelerators occurs in pulses that cause the diode output current to be pulsed. The total charge in a radiation current pulse must not be so large as to cause the feedback capacitor voltage to exceed the op-amp supply voltage. To test whether this might occur under clinical use, compare the diode response per unit dose at the smallest SSD expected for use (e.g., 70 cm) with that at SSD of 100 cm. If the diode response per unit dose at the smallest SSD is lower than the response at the larger SSD position (contrary to what is expected from the instantaneous dose-rate dependence discussed in section 2.2.1), then the charge-per-pulse limit of the electrometer has been exceeded.

An advantage of CPC electrometers is that an unlimited dose can be accumulated per measurement. There is no shorting requirement of the capacitor because the charge pulse keeps the capacitor cleared of charge.

2.4.1.2 ADC electrometers

An ADC electrometer converts the voltage across the feedback capacitor to a digital value which is then displayed. The feedback capacitor is generally much larger than the one in a CPC electrometer because it must hold all the charge accumulated during the treatment. After the measurement is completed, the charge is cleared with a shorting switch so that another measurement can be made. There are no limits on the dose per pulse or average dose rate because there is very little change in voltage per pulse on the large capacitor of the ADC electrometer. However, the amplifier supply voltage and the digital display limit the maximum dose per measurement.

2.4.2 Compatibility with diode polarity and sensitivity

Electrometers designed for diode in vivo dosimetry generally display the measurement as a dose value. To achieve this, the electrometer display is cali-

brated by either microprocessor control or potentiometer adjustment. It is therefore important that the electrometer have the adjustment range to accommodate both the initial diode sensitivity and later, radiation-induced sensitivity changes. Electrometers with microprocessor or computer controlled adjustments can usually handle this range of sensitivities, while electrometers that use a potentiometer adjustment are normally designed for a specific diode detector type and have a narrower range of adjustment.

Electrometers designed for in vivo dosimetry are often unipolar and can only measure charge of one polarity. This means that the diode detector polarity must be matched to the electrometer. Bipolar electrometers can measure both polarities and thus can be used with diode detectors of either polarity. However, diode dosimetry does not require a bipolar electrometer because, unlike ionization chambers, the diode signal polarity cannot be changed during use.

CAUTION: Some ADC type electrometers have supply voltages that take the display full scale in the direction of the intended polarity, but allow only a partial use of the display in the direction of the opposite polarity. If the wrong polarity diode detector is used with this electrometer, measurement errors can occur if the dose measured exceeds the supply voltage limit and no warning of a dose-display limit is given.

2.4.3 Input offset voltage, series resistance, and diode impedance⁴⁶

By ionization chamber standards, the diode impedance is not very high. For example, the typical impedance of an ionization chamber is $10^{12} \Omega$ (guard-to-collection electrode), while that of a diode is on the order of $10^8 \Omega$. As a result, an electrometer with a moderate input offset voltage can cause a significant leakage current in the diode because that input offset voltage is applied directly across the diode.

Equation (1) calculates the maximum input offset voltage of the electrometer, $V_{IN_{Max}}$, at which the leakage current is no more than a fraction f of the average signal current $DR_{Min} \cdot S_{Diode}$:

$$V_{IN_{Max}} = (f \cdot S_{Diode} \cdot DR_{Min} / 60) \cdot R_{Diode} \quad (1)$$

where DR_{Min} = minimum average accelerator dose rate (cGy/min)

S_{Diode} = charge sensitivity of the diode (nC/cGy)

R_{Diode} = impedance of the diode.

For example, if a diode with an impedance of $100 \text{ M}\Omega$ and a sensitivity of 0.4 nC/cGy is used to measure the dose in a beam with an average dose rate of 60 cGy/min , then for the leakage contribution to be $<0.1\%$ of the signal ($f = 0.001$), the input offset voltage maximum should be $40 \mu\text{V}$ or less. Many ionization chamber electrometers are not specified to maintain

such a low input offset voltage because input offset does not contribute significant leakage in an ion chamber. Leakage is of particular concern when diodes are used in low average dose rate situations such as TBI or for out-of-field dosimetry.

It is worth noting that the diode impedance is defined as the ratio between the applied bias voltage and the resulting electrical current.⁴⁶ The current is zero at zero bias voltage. Therefore, diode impedance has to be measured at a specified bias voltage, such as 10 mV.

Another common feature of electrometers is the use of a series resistor in the input of the electrometer to protect the input from damage due to electrical shock. The radiation current from the diode causes a voltage across this resistor that forwardly biases the diode and consequently generates a leakage current. If the values of this series resistance and the offset voltage are reasonably small, the ratio between the leakage current and the radiation current is equal to the ratio between the series resistance and the diode impedance. For example, a 50 k Ω series resistor would result in a 0.5% leakage noise-to-signal ratio for a 10 M Ω diode. Therefore, it is better that the series resistance is <10 k Ω for an electrometer used in diode in vivo dosimetry.

Note that all electrometers are, by their nature, very high input impedance devices, easily exceeding 10¹² Ω . This impedance is not to be confused with an input resistance placed in series between the input and the detector.

In summary, the user should understand the characteristics of any electrometer that is used as part of the diode in vivo dosimetry system and should reach a clear understanding with the vendor about the desired characteristics of newly purchased electrometers.

3 FACTORS TO CONSIDER BEFORE PURCHASING A DIODE IN VIVO DOSIMETRY SYSTEM

Purchase specifications for a diode-based in vivo dosimetry system depend on both the intended pattern of clinical use and available resources. Table I summarizes the commercial systems available in 2003 and their primary vendors. Since systems change, potential users should seek up-to-date information directly from the vendors. Table II outlines system features about which the vendor should be able to supply information. The ESTRO report²⁴ and section 13 of this report and references listed therein describe organizational features of some successful diodes in vivo dosimetry programs.

3.1 Components of a system for measurements at conventional treatment distances

If the goal is to perform in vivo measurements at conventional treatment distances (patient on treatment couch) for some or all patients, the optimal arrangement at each treatment unit includes:

Table I. Diode in vivo dosimetry systems available as of fall 2003
(After reference 108).

Company	Electrometers	Diode Detectors		
		Name	Type of die	Energy Range
Capintec	2 BASIC (2 channels)	5230-2135	p	1-4 MV
		5230-2137	p	4-25 MeV electron
		5230-2139	p	6-12 MV 15-25 MV
Cardinal Health Radiation Management Services (products formerly sold by Nuclear Associates and InVision)	VeriDose 5 (5 channels)	VeriDose 30-471	n	1-4 MV
		VeriDose 30-472	n	5-11 MV
		VeriDose 30-473	n	12-17 MV
		VeriDose 30-474	n	18-25 MV
		VeriDose 30-475	n	5-25 MeV electron
PTW	VIVODOS (4 channels, expandable to 12 channels)	T60010L	p	⁶⁰ Co - 4 MV
		T60010M	p	5-13 MV
		T60010H	p	13-25 MV
		T60010E	p	Electrons (4-30 MeV)
Scanditronix Wellhöfer	DPD 3 (3 channels) or DPD-12 (12 channels) or InViDos (12 or 24 channels)	EDD-5	p	organs at risk
		EDP-5	p	cobalt-60
		EDP-10	p	4-8 MV
		EDP-15	p	6-12 MV
		EDP-20	p	10-20 MV
		EDP-HL	p	≥16 MV
Sun Nuclear	1333 rf-IVD or 1135 IVD Solutions (3 channels, expandable to 27 channels)	QED 111300	p,n*	Skin and 70 kV and up
		QED 111400	p,n*	1-4 MV
		QED 111500	p,n*	6-12 MV
		QED 111600	p,n*	15-25 MV
		QED 111200	p,n*	electrons
		ISORAD-3 1162000	n	1-4 MV
		ISORAD-3 1163000	n	6-12 MV
		ISORAD-3 1164000	n	15-25 MV

*QED diodes from 1997 through 2002 use p-type die; QED diodes from 2003-on use n-type die.

Table II. In vivo diode dosimetry system parameters and features to ask the vendor about.

Parameter	Units	Recommended Test Conditions	Features of Interest
Sensitivity	nC/cGy or nC/Gy	—	Lowest sensitivity the electrometer can take, especially for TBI or TSET where the beam intensity is much lower.
SVWAD	%/kGy	The SVWAD tested at beam energy ≥ 10 MeV electron or ≥ 15 MV photon should be provided.	Pre-irradiation with beam energy ≥ 10 MeV or radiation hardening by other methods.
SSD or dose per pulse dependence	%	Diode placed on the phantom surface with no additional buildup. SSD dependence determined according to the methods of section 6.1.1.	Different accelerators may have quite different dose per pulse for the same SSD range, even for the same energy.
SVWT	%/°C	Measured under thermal equilibrium, at a stated beam energy.	Automatic compensation for the temperature dependence, useful for TBI or TSET.
Directional dependence	%	Diode placed on a solid phantom with the typical clinical thickness, such as 6 cm (see Fig. 4).	Shape of the diode (flat or cylindrical).
Buildup thickness	g/cm ²	Converted to water-equivalent thickness.	Sufficient to the intended energy range to shield the contaminant electrons.
Output polarity	—	—	Automatic detection of the diode polarity and instant adjustment.
Type of output	—	—	Hard copy or electronic copy, or both.
List of journal publications	—	—	Publications dealing with current models of particular interest.
Interface with any R & V system	—	—	—

1. At least one photon diode with a specified energy range that includes the beam to be measured (e.g., for a 6 MV and 15 MV dual photon energy linac, one diode for each energy). See section 2.3 for the physical rationale for preferring diodes with buildup matched to the beam energy. Two diodes per beam energy and an electrometer with at least two channels are helpful for combined entrance and exit dosimetry. If budgetary or other constraints limit photon diodes to one type per dual energy machine, diodes designed for use at the higher energy are strongly preferable so that contaminant electrons do not introduce extra field size or SSD dependences.^{61,62}
2. A minimal buildup diode designed for electron in vivo dosimetry. Because of the severe underdose (>20%) beneath a photon diode used in an electron beam, TG-62 strongly advises that this (purchased if necessary). Photon diodes should not be used.
3. An electrometer designed for use with in vivo dosimetry diodes. Section 2.4 describes problems that can arise due to mismatch between the electrometer and its intended use. The vendors of in vivo dosimetry diodes also sell electrometers and the physicist should consider the convenience of purchasing a package.
4. A system output including visual display, hard-copy capability and a computer (PC) interface; these features are currently provided by most vendors. Because an interface to the record and verify system is very helpful,⁶³ users are advised to check availability with vendors.

3.2 Additional features for TBI measurements

TBI measurements place additional requirements on the system, including:

1. *Low leakage current* (see section 2.4.3): The leakage current from all system components (electrometer and diodes) should be low enough to allow accurate readings at the low average dose rates at typical TBI treatment distances. The ratio of leakage to radiation-induced current at source-diode distances over 300 cm is 10 or more times greater than at 100 cm and leakage is increased further if prolonged contact raises the diode temperature. A good diode in vivo dosimetry system for TBI has low electrometer offset voltage (<10 μ V) and high diode impedance (>100 M Ω) and/or automatic leakage current subtraction.
2. *Small SVWT (temperature dependence)* (see section 2.2.3): Because of the long contact time on the patient, the diode SVWT should be as small as possible to minimize the impact of the temperature correction. It would be best for the in vivo dosimetry system to automatically correct for SVWT and this feature has recently become commercially available.
3. *Number of diodes*: To check dose uniformity over the body for TBI, six to eight photon detectors, all rated for the same beam quality and a multi-channel electrometer and display, are needed. If the TBI protocol includes

a chest wall electron boost at conventional SSD, an electron diode is also recommended.

4. The *integral buildup* should be appropriate to the beam energy (see section 2.3.5). Large treatment distance, the use of a beam spoiler, and the presence of light clothing or blankets all contribute contaminant electrons which will affect the readings of diodes with insufficient buildup. On the other hand, many TBI protocols require in vivo dosimetry at each treatment session. Buildup that is too thick for the beam energy produces greater underdose below the diode. For a diode designed for 15 to 18 MV photon beams used in a 6 MV beam, the dose shadow at shallow depths can exceed 25% and at 10 cm, can exceed 10%.⁶¹ Without deliberate efforts to change the diode position at each session, the diode will shadow the same volume at each treatment.
5. A *stable mounting* to keep the in-room electronics out of the direct beam or a cable-free system.

3.3 Additional general features

Further features to consider for either conventional distance or TBI measurements include:

1. The *diode shape* may be cylindrical, hemispherical, or a similar shape with one flat and one curved side (see section 2.3.1). Hemispherical diodes are easier to place on flat anatomy and are preferable for exit dosimetry, but cylindrical diodes have much weaker angular dependence, making them preferable for fields incident at oblique angles (e.g., tangents).
2. *Reduced need for manually applied correction factors*: Consult both the vendor's product specifications and recent publications for information about the detector's instantaneous dose-rate or dose per pulse dependence (see section 2.2.1). Small instantaneous dose rate dependence may make SSD and treatment accessory correction factors unnecessary. Investigate the availability of automatic temperature correction.
3. *Adequacy of buildup* (especially for photon beams >15 MV): Consult vendor's literature to see if the intrinsic buildup is sufficient ($\sim d_{\max}$ for a 10×10 cm² field for the beam). Contaminant electrons increase the need for correction factors and complicate interpretation of in vivo readings.
4. *Multiple calibration factors*: If you plan to use a single diode under several qualitatively different conditions (e.g., entrance and exit dosimetry or different beam energies), understand how the system handles multiple calibration factors. Vendor's specifications and/or discussions with potential vendors are helpful.
5. *Electrometer limitations* (see section 2.4): Is there a maximum displayed dose per measurement; if so, are you likely to exceed it? Are the polarities of the electrometer and diodes compatible?

6. *Long-term stability (SVWAD)* (see section 2.2.2): Estimate the rate at which diodes in your practice will accumulate dose and use vendor's information to estimate the impact of SVWAD on your in vivo dosimetry program.
7. *P-type or n-type* (see section 2.2.4): Both types are available and selection should be based upon the manufacturer's current published specifications. The diode type (p or n) should not be the determining factor because the type alone does not determine clinical performance characteristics.^{1,14,31,37}
8. *Support and storage*: Will extra cabling and/or "home-built" support devices be needed to facilitate convenient use and storage? At least one vendor provides a "wireless" in vivo diode dosimetry package.
9. *Overall specifications*: If possible, check whether the manufacturer's specifications are tighter or more lenient than the acceptance criteria discussed in the next section.
10. *Sharing equipment?* It is best to avoid routine sharing of pieces of the in vivo dosimetry system (diodes, electrometers, printers) between treatment units to prevent scheduling conflicts and damage to the equipment.

4 ACCEPTANCE TESTING

Before embarking on the labor-intensive measurements of calibration and correction factors, simpler acceptance tests of a new diode in vivo dosimetry system are recommended. The acceptance tests and criteria suggested below are general rather than specific to a particular system. If manufacturer's specifications are significantly different from these, it is recommended to add them or substitute them for the generic acceptance criteria below (see also section 3.3, #9). For the acceptance tests, it is not necessary to use the beam energy for which the diodes were designed—e.g., with a multichannel electrometer, 6 MV and 15 MV diodes can be tested together. Tests 2 to 5 are also recommended to accept a new diode into a previously commissioned system. Since problems with new electrometers can be discovered at this point, it is advisable to read section 2.4 of this report when planning the acceptance testing. TG-62 strongly recommends keeping a written record of all acceptance and commissioning measurements.

1. *Overall system integrity*: Assemble the system at an accelerator, connected as it would be for clinical use. Fasten the diodes securely to a flat entrance surface (e.g., 5 to 10 cm thickness of plastic phantom) at a convenient SSD (e.g., SSD=100 cm) in a field large enough to include all the diodes within the central (flat) 80% of the field, with the beam at direct, vertical incidence. Keep any in-room electrometer out of the direct beam. While performing tests 2 to 5, observe and check the performance of all the output features including the display and printer.

2. Post irradiation signal drift: Arm the unit for measurement and irradiate it with 100 MU. Note the display reading immediately after the irradiation terminates. Keep the unit in measurement mode and observe the change in display for 1 minute—the change should be less than 0.5%.

For tests 3 to 5, it is advisable to simultaneously irradiate an ion chamber to confirm accelerator output constancy during the tests.

3. *Short-term reproducibility*: For each diode, record the readings for ten exposures of 100 MU each. For each diode, the coefficient of variation (standard deviation/average) should be <1%.

For the next two tests, it is assumed that the accelerator output linearity with MU and the extent to which dose/MU depends on average dose rate (MU/min) have been confirmed with an ion chamber during routine accelerator QA procedures. If differences exceeding 1% are seen in the diode responses (especially if several diodes are being tested together and behave similarly) and an ion chamber has not been simultaneously irradiated, recheck these aspects of the accelerator output before assuming that the problem lies with the diode system.

4. *Dependence on average dose-rate*: If the accelerator output (dose/MU) does not vary with average dose rate, the diode readings/MU should not vary. For each diode, record the readings for five exposures of 100 MU each at the minimum average dose rate (MU/min) in clinical use and average the readings. Then record the readings for five 100 MU exposures at the maximum MU/min in clinical use and average these readings. The ratio of the average reading at maximum to minimum MU/min should be between 0.98 and 1.02. See section 2.4.1.1 (CPC electrometers) for a possible cause of a larger discrepancy.
5. *Dose linearity*: For each diode, record and average the readings for five exposures at ~20 MU (or the lowest MU expected for in vivo dosimetry) to obtain Average (Min MU). Record and average the readings for five exposures of the same field at the highest MU expected for in vivo dosimetry to obtain Average (Max MU). Keep the MU/min constant. The ratio

$$\frac{\text{Average (Max MU)}}{\text{Average (Min MU)}} \div \frac{\text{Max MU}}{\text{Min MU}}$$

should be between 0.98 and 1.02.

6. *TBI tests*: see section 11.

Problems or questions raised by acceptance measurements should be resolved before proceeding with calibration, correction factor measurements, and clinical use. If you cannot isolate the problem, consult with the vendor's technical sup-

port group and provide them with relevant supporting data. Only if such discussions confirm the problem should the system be returned for repair.

5 CALIBRATION

The first step in commissioning a new system or a new diode for clinical use is to measure a calibration factor for each diode. The calibration relates to the combination of diode and electrometer, and changing either the electrometer or the diode requires a new calibration.

Although the diode is irradiated on rather than *inside* a solid surface, its reading is proportional to the dose at points of interest within the phantom or patient. Calibration relates the diode readings under reference conditions of field size and SSD to the dose at a chosen point within a water phantom—the diode dosimetry reference point (DDRP). The reference point and reference conditions for diode dosimetry may differ from the beam calibration reference point and conditions. For further discussion of the depth of the DDRP, see section 5.1.1. The diode dosimetry reference field size and SSD are often chosen to be typical of clinical use conditions rather than the conditions required by TG-51.⁶⁴

The diode calibration factor is defined as the ratio of $D_w(cal)$, the dose to water at the DDRP under the diode dosimetry reference conditions, to $R(cal)$, the diode reading, for the same MU and under the same reference conditions. This definition is consistent with the ESTRO reports.^{14,24}

In general, $D_w(cal)$ is determined from ion chamber measurements and clinical beam data. Section 5.1.2 describes the use of clinical beam data to relate linac beams calibrated according to TG-51 and diode dosimetry calibrations using different reference conditions, such as d_{max} for the depth of the DDRP.

The calibration factor, F_{cal} , is given by

$$F_{cal} = \frac{D_w(cal)}{R(cal)}, \quad (2)$$

or alternatively, by

$$F_{cal} = \frac{\frac{D_w(cal)}{MU}}{\frac{R(cal)}{MU}}. \quad (3)$$

The two definitions give numerically and dimensionally identical results, but they are conceptually different in that equation (3) permits the use of different

MU for the ion chamber and the diode irradiations. The dimensions of F_{cal} are dose/reading (units of cGy/reading or Gy/reading), where the electrometer-user interface determines the units of the reading, R. For electrometers designed for in vivo diode measurements, the calibration factor is often imbedded in the system's display, so the display reads directly as "dose." In such cases, the user either adjusts a potentiometer so that the display agrees with the measured dose at the DDRP or inputs this dose to a computer that calculates and stores the calibration factor. Because systems with a potentiometer usually allow only one adjustment, their readings are the dose represented by the diode response under one set of reference conditions. The dose for other reference conditions is obtained by multiplying the display value by a measured correction factor; as an example, see section 6.1.2. In vivo dosimetry systems with a computer interface are more flexible and often allow several calibration factors to be saved for a single diode so that doses corresponding to different calibration conditions can be displayed by menu choice.

We will denote the diode dosimetry reference conditions by an additional subscript of the corresponding calibration factor: $F_{\text{cal, en}}$ and $F_{\text{cal, ex}}$, for entrance and exit dosimetry, respectively, at typical treatment distances and $F_{\text{cal, TBI}}$ for TBI entrance dosimetry. If a single diode is used in qualitatively different ways, either separate calibration measurements can be made for each use condition or a single calibration factor can be obtained, and correction factors (see section 6) can be measured and applied for the other conditions. In section 5.1, we discuss calibration for entrance dosimetry at typical treatment distances, (SSD between approximately 70 cm and 130 cm for photons, or cone-in-contact with patient to SSD of 110 to 115 cm for electrons). In section 5.2, we discuss calibration for exit dosimetry at similar distances. Calibration methodology for TBI distances is conceptually similar and is discussed in section 11.

Because the diode calibration factors link the diode radiation response to the absolute dose calibration of the therapy machine, it is important to maintain a complete and coherent record of the beam, phantom, and temperature conditions that exist during calibration.

5.1 Entrance calibration factor, $F_{\text{cal, en}}$

5.1.1 Calibration conditions

Phantom material: Because in vivo dosimetry diodes are usually not waterproof, most reports recommend calibrating diodes on plastic phantom material to provide backscatter similar to in vivo.^{1,3,5,6,20,24,34,62,65,66,67,68,69,70} Below, we assume that the diodes are calibrated on the surface of a plastic phantom. Figure 5(a) diagrams a typical entrance calibration setup. Suitable phantom dimensions are approximately 25×25 cm² in area and approximately 10 cm thickness. Polystyrene or solid water are preferable but, since the phantom is used only to provide backscatter, other plastics can be used. Many clinics have a plastic

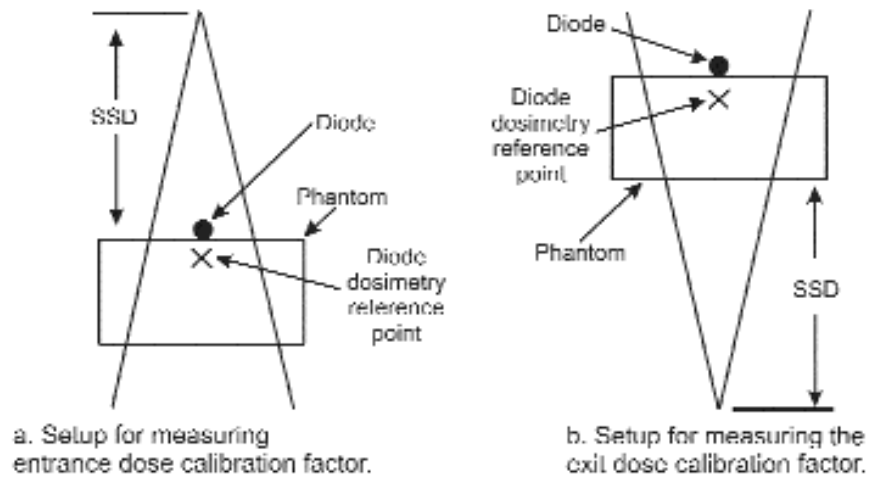


Figure 5. Schematic diagrams for entrance (a) and exit (b) dose calibration factors.

phantom for routine relative dosimetry and/or output constancy checks, and this is also suitable for diode calibration. It should be noted that alternative techniques have been successfully applied; See reference 44 for in-air calibration methods.

Diode dosimetry reference point: In the majority of publications on diode in vivo dosimetry for photons, the DDRP is on the central axis at depth of d_{max} for moderate field sizes (10×10 to 15×15 cm²) in water-equivalent material (as representative examples, see references 3, 4, 5, 14, 24, 65, and 70. Below we refer to this depth as “ d_{max} ” without further discussion of field-size effects on the buildup region. This depth, which is different for different beam energies, is approximately equal to the effective thickness of the buildup surrounding the die for a diode used in its rated energy range (see section 2). If the DDRP is at d_{max} , the calibrated diode reading represents the traditional “entrance dose,” and comparison with much of the in vivo dosimetry literature is simplified. However, considerations such as more accurate dosimetry modeling at a deeper depth by the treatment planning system or the direct relationship of 10 cm depth to the TG-5164 high-energy photon beam calibration may lead a user to prefer a deeper DDRP.

Diode dosimetry reference beam geometry: Because in vivo dosimetry is not a primary dose-calibration procedure, the user has flexibility in choice of reference conditions. Commonly used collimator reference settings for photon entrance in vivo dosimetry calibration are a 10×10 , 15×15 cm², or a collimator setting typical of clinical field sizes. Commonly used SSD reference conditions include:

1. Isocenter is coincident with phantom surface (SSD=100 cm for most linacs).

2. Isocenter is at the depth of the DDRP.
3. The SSD is representative of clinical use (e.g., SSD=90 cm) to reduce the need for SSD corrections to the diode reading.^{34,65}

Choosing reference conditions typical of clinical conditions may be less important for the current generation of photon diodes, as vendor's specifications indicate small SSD dependence (<1% to 2%) for diodes used within their stated energy range.

For electron in vivo dosimetry, if the majority of treatments are at SSD=100 cm, method (1) is recommended (SSD=100 cm, 10×10 or 15×15 cone) although use of other SSD is reported in the literature.⁷¹

5.1.2 Determining the dose at the DDRP for entrance dosimetry

The task group recommends checking the accelerator output for constancy using the clinic's TG-40-recommended monthly check procedure immediately before beginning diode calibration. The constancy check is "performed by a physicist with an ionometric dosimetry system that is acceptable for calibration by an Accredited Dosimetry Calibration Laboratory"^{12(p.592)} and the appropriate temperature/pressure corrections are applied.^{12(p.589)} The diode calibration is then "slaved" to the results of the constancy measurement. Of course, if the physicist corrects the accelerator output before proceeding, the diode calibration is slaved to the results of the final, confirming constancy measurement.

As an example, suppose the TG-51 calibration of a linac photon beam with 100 cm source-to-isocenter distance (SID) is performed with a 10×10 cm² collimator setting at SSD=100 cm. Suppose the diode dosimetry reference conditions are reference depth of d_{max} , phantom at SSD=90 cm and collimator setting of 15×15 cm². Suppose also that d_{max} is the reference depth for the clinical dosimetry data tables [the phantom scatter factor, S_p is determined at d_{max} , TMR (tissue-maximum ratio) rather than TPR (tissue-phantom ratio) used] and that the dosimetry calculation data such as the percent depth doses (PDDs) are acquired at SSD=100 cm. Finally, suppose that $D_{w,0}/MU$ is the dose per MU to water at the TG-51 reference point under TG-51 reference conditions as determined by the constancy check. The corresponding dose per MU to water for the diode entrance dosimetry calibration reference conditions, $D_{w,en}(cal)/MU$, is calculated from the clinical beam data:

$$\frac{D_{w,en}(cal)}{MU} = \frac{D_{w,0}}{MU} \cdot \left[\frac{100}{PDD(10 \times 10, 10)} \right] S_c(15 \times 15) S_p(13.5 \times 13.5) \left[\frac{100 + d_{max}}{90 + d_{max}} \right]^2. \quad (4)$$

As an approximation, S_p is evaluated for the field size at the surface rather than at SSD+ d_{max} . If the constancy check measurements show that $D_{w,0}/MU$ is 1% high, $D_{w,en}(cal)/MU$ reflects that result.

For electrons, a similar calculation involving cone factors (and airgap factors, depending on the SSD) would be made. With this process, the dose per MU at the DDRP is determined in a manner that is both practical and traceable to the TG-51 beam calibration.

5.1.3 Entrance calibration measurements

1. Perform the TG-40 monthly constancy check.
2. Fasten the diode(s) securely to the phantom entrance surface, not in any special calibration fixture. The entire length of a cylindrical diode or the flat side of a hemispherical diode should be in direct contact with the phantom. No additional buildup should be placed over the diodes unless the diode's intrinsic buildup is insufficient and will be supplemented by a permanent buildup cap in vivo.^{21,51,72} Several diodes rated for the same beam quality and connected to independent electrometer channels can be calibrated simultaneously in a single beam, providing the diodes are all within the flat, inner 80% of the field, at least 2 cm from any field edge, and approximately 1 cm from a neighboring diode to reduce the effect of secondary photon or electron scatter on the diode readings.

Many authors, including references 3, 14, 24, and 65, describe calibration with simultaneous ion chamber and diode measurements, and the diodes shifted slightly so they do not shadow the chamber. Most of these papers, which predate TG-51, place the chamber on axis at d_{\max} and determine the dose at the DDRP from the corrected chamber readings (e.g., with TG-21 correction factors). A further justification for this methodology given in many European papers^{14,24} is that it accounts for unexpected linac output fluctuations.

3. Because of the diode SVWT, record the phantom temperature at calibration to allow for temperature corrections in vivo. (Reference 45 reports equilibration half-times of 0.5 to 1.5 minutes and full equilibration times of 10 minutes to an ~ 31 °C skin temperature). If temperature correction is of particular concern, consider raising the linac room temperature to 25° to 27 °C during the calibration or calibrating the diodes in contact with a warmed surface, as described in references 24, 45, and 72.
4. If the diode reading is R for M MU, $F_{\text{cal,en}}$ is determined from equations (4) and either (2) or (3).
5. Because individual diode sensitivities differ, it is common for each diode to have a different $F_{\text{cal,en}}$.
6. Determine a separate calibration factor for each beam energy at which a diode will be used.
7. Entrance calibration factors for photon and electron diodes are measured in the same way.

5.2 Exit calibration factor, $F_{\text{cal,ex}}$

If the diode system will also be used for exit dosimetry, many physicists measure an exit calibration factor, $F_{\text{cal,ex}}$,^{3,14,34,62,65,73} since scatter conditions, dose per pulse, and diode position relative to the reference point are different for entrance and exit dosimetry. An alternative approach is to determine an exit dose correction factor (see section 6).

5.2.1 Exit calibration conditions

The phantom can be irradiated through the radiolucent couch insert from directly below the couch with the diodes on the top (exit) surface [figure 5(b)] or a vertical phantom may be irradiated by a horizontal beam.³ Exit diode dosimetry reference conditions include the SSD, the collimator setting, and the phantom thickness, t_{cal} . Exit dosimetry for other thicknesses is dealt with through thickness correction factors (see section 6.3). The most common DDRP for exit in vivo dosimetry is on the central axis at d_{max} “upstream” of the exit surface (depth of $t_{\text{cal}} - d_{\text{max}}$) as shown schematically in figure 5(b)^{3,62,65,73}. Various SSD choices are reported including SSD=100 cm,^{3,73} or an exit calibration SSD and phantom thickness which are typical of clinical condition.³⁴ The same temperature considerations apply as for entrance calibration.

5.2.2 Determining the dose to water at the diode exit-dosimetry reference point

The dose at the exit DDRP under the reference conditions can be inferred from the ion chamber output constancy measurement of $D_{\text{w,0}}/MU$ (section 5.1.2) and the clinical beam data.

As an example, suppose the diode exit dosimetry reference conditions are SSD=90 cm, collimator setting 15×15, phantom thickness $t=20$ cm, and the exit DDRP is on the central axis at d_{max} upstream of the exit surface, and suppose the clinical PDD tables were acquired at an SSD of 100 cm. Then

$$\frac{D_{\text{w,ex}}(\text{cal})}{MU} = \frac{D_{\text{w,0}}}{MU} \cdot \left[\frac{PDD(13.5 \times 13.5, 20 - d_{\text{max}})}{PDD(10 \times 10, 10)} \right] S_c(15 \times 15) S_p(13.5 \times 13.5) \cdot \left[\frac{100 + d_{\text{max}}}{90 + d_{\text{max}}} \right]^2 \cdot F. \quad (5)$$

Here F is the Mayneord F factor connecting the PDD at SSD=100 and SSD=90 cm. If the diode reading for M MU is $R_{\text{ex}}(\text{cal})$ then $F_{\text{cal,ex}}$ is determined from equations (5) and (2) or (3).

Exit dosimetry calibration using the clinical PDD or TMR data to determine $D_{\text{w,ex}}(\text{cal})/MU$ relates the diode reading to the exit dose with full backscatter. This facilitates comparison with hand calculations and the calculations of most treatment planning systems, but the true dose, as measured with an ion chamber at the exit DDRP, may be several percent lower.^{52,74,75} Some papers describe

calibrations which measure the exit dose with an ion chamber at depth ($t_{\text{cal}} - d_{\text{max}}$). To improve comparison with calculated exit doses, these authors apply a correction factor to account for the loss of backscatter⁷⁶ or make the ion chamber measurements with full backscatter.³⁴

5.2.3 Positioning considerations for exit-dosimetry calibration

If the phantom contains an ion chamber, either the diodes are shifted slightly off-center to avoid its shadow or the chamber is replaced by a solid slab to prevent perturbation of the exit photon fluence. The diodes should be positioned on the exit surface, placed exactly as for entrance calibration. This is also how they should be positioned for in vivo measurements. It is important that the flat side of a hemispherical diode be in contact with the phantom because there is minimal buildup on the *flat* side and approximately d_{max} of buildup on the curved side. Placing hemispherical diodes incorrectly can result in a measurement error of up to 10%.

6 CORRECTION FACTORS

Correction factors account for changes in the diode response when measurement and calibration conditions are different. The corrections made in an individual clinical practice depend on the accuracy desired from in vivo dosimetry, the diode system used, and the treatment techniques that will be monitored. TG-62 advises that even if one does not intend to use correction factors clinically, they should be spot-checked when the diode system is commissioned so that their effects are understood and their omission can be justified.

The correction factor for a change of variable X from calibration conditions, (cal), is defined by

$$CF_x = \frac{\frac{D_w(X)}{R(X)}}{\frac{D_w(cal)}{R(cal)}} , \quad (6)$$

or equivalently, by

$$CF_x = \frac{\frac{D_w(cal)}{R(X)}}{\frac{D_w(cal)}{R(cal)}} . \quad (7)$$

Here $D_w(X)$ is the dose to water at the DDRP under conditions X (e.g., SSD, field size, temperature) which differ from calibration. $D_w(X)$ is either inferred from clinical beam data or measured as part of the diode commissioning with an ion chamber placed at the DDRP under conditions X . $R(X)$ is the diode reading under conditions X , and $D_w(cal)$ and $R(cal)$ are the corresponding quantities under calibration conditions. Note that the denominator of equation (6), $[D_w(cal)/R(cal)]$, is the calibration factor, F_{cal} . The dose to the DDRP, $D_{diode}(X)$, which is inferred from the diode reading $R(X)$ made under conditions X , is given by

$$D_{diode}(X) = CF_X \cdot F_{cal} \cdot R(X) . \quad (8)$$

We follow the same convention in defining the correction factors as ESTRO.²⁴ Accordingly, conditions which increase the diode sensitivity relative to calibration conditions have correction factors which are less than unity. Note that some of the literature uses “diode response factors” which are the inverse of these correction factors.^{65,77}

There are three classes of correction factors—beam-dependent factors (correction for SSD, field sizes, or beam modifiers), intrinsic factors (correction for temperature or diode orientation), and factors that depend on patient variables (e.g., body contour or thickness). We denote the beam and phantom correction factors as C_i (e.g., C_{SSD} for SSD correction factor) and the intrinsic response correction factors by K_i (e.g., K_T for the temperature correction factor). It is assumed that the correction factors are independent of each other—for example, that the field-size correction factors measured at two different SSD are equal within measurement uncertainty. If this is the case, when measurement and calibration conditions differ in several ways, involving n_1 beam-dependent factors, (X_1, \dots, X_{n_1}) , and n_2 intrinsic factors (x_1, \dots, x_{n_2}) , D_{inf} is given by

$$D_{inf}(X_1, \dots, X_{n_1}, x_1, \dots, x_{n_2}) = \left[\prod_{i=1 \rightarrow n_2} K(x_i) \prod_{j=i @ n_1} C_j(X_j) \right] F_{cal} R(X_1, \dots, X_{n_1}, x_1, \dots, x_{n_2}) . \quad (9)$$

Since field size, SSD, and beam modifiers all change the instantaneous dose rate, such independence is only approximate. However, the successful use of equation (9) in numerous clinical applications of in vivo dosimetry (including those in our references) suggests that the approximation is good. Measurements confirming the independence of field size and SSD correction factors for Scanditronix EDP-20 and EDP-30 diodes at 18 MV and 25 MV are reported in the ESTRO report.²⁴ Measurements by a member of TG-62 (DK) for n- and p-type Isorad diodes at 18 MV demonstrate independence of wedge and SSD correction factors. On the other hand, recent work⁴³ demonstrates that

SVWT varies with the instantaneous dose rate for diodes with insufficient pre-irradiation.

Vendors provide product-specific information about some of the characteristics discussed below. However, correction factors intended for clinical use should be measured for each diode because they may be different even for diodes from the same manufacturing batch.^{4,65,73} Correction factors from other users, vendors, or the literature should not be substituted. If one's measurements confirm that it is sufficiently accurate to apply an average correction factor for a class of treatment fields (e.g., an average SSD correction for all prostate fields at 15 MV)^{21,65} or for a batch of "identical" diodes at one beam energy^{3,37,51} the simplification is worthwhile.

Older diodes and diodes used outside their specified energy range may require larger correction factors than current vendor-specified values. Often, correction factors that differ greatly from unity indicate a defective diode. While TG-62 recommends using diodes within the energy range for which they were designed, some publications document the successful use of diodes rated for high megavoltage photons in lower energy beams.⁶¹ Of course, these diodes must be calibrated separately for the energies of use.

The most important correction factors are discussed below for treatments at conventional SSD; correction factors for TBI are discussed in section 11. The same precautions should be taken for correction factor measurements as for calibration, including careful diode positioning, known phantom temperature, and confidence in beam characteristics based on recent routine accelerator QA. It is assumed that the response linearity of the diode system was established at acceptance.

6.1 Beam-dependent correction factors

6.1.1 Entrance SSD correction factor, C_{SSD}

The setup for determining the entrance SSD correction factor, C_{SSD} , is identical to that used for entrance dose calibration [section 5.1 and figure 5(a)] except that measurements are made at different SSD, covering the range expected during treatment. The same procedure is used for photons and electrons. The collimator (or cone/insert) is kept at the calibration reference size. The correction factor is given by

$$C_{SSD} = \frac{\left(\frac{D_w(SSD)}{R(SSD)} \right)}{\left(\frac{D_w(SSD)_{cal}}{R(SSD)_{cal}} \right)} = \frac{\left(\frac{D_w(SSD)}{R(SSD)} \right)}{F_{calen}}, \quad (10)$$

where SSD_{cal} is the diode calibration SSD. Three effects contribute to C_{SSD} . One is the purely geometric effect of the different distances from source to ion chamber and source to diode. One is the instantaneous dose-rate or dose-per-pulse dependence of diode response described in section 2.2.3. The third effect, important for diodes with inadequate buildup, is dose from contaminant electrons. Thus, the magnitude and range of variation of C_{SSD} depend on the overall structure of the diode, including n-type or p-type, level of doping, and history of radiation damage, and thickness and material of buildup.^{37,51,78} Some publications^{37,44,48} isolate the dose-per-pulse dependence by placing the diode under extra buildup or by changing the gun current to vary the dose per pulse. However, the clinical C_{SSD} includes all three effects and should be measured with the diode exposed to the beam as it is for in vivo dosimetry. As an example, figure 6 shows measured C_{SSD} values for six modern photon diodes, all used within their designed energy ranges [source-to-detector distance (SDD)=SSD].

Although some reports state⁵⁶ that C_{SSD} for electrons is close to unity, individual users should check literature statements with their own measurements.

Many papers on diode in vivo dosimetry describe measurements and magnitudes of C_{SSD} . These include references 3, 5, 6, 24, 34, 37, 44, 60, 65, 77, and 78 for photons and 45, 56, 65, and 66 for electrons.

6.1.2 Exit dose as a correction factor, $C_{ex,std}$

Rather than using a separate exit dose calibration factor, $F_{cal,ex}$, some workers express the dose at the exit DDRP under exit diode dosimetry reference conditions by means of a multiplicative correction factor applied to $F_{cal,en}$.⁶⁵ The same diode measurements are made as are described in section 5.2 and $D_{w,ex}(cal)$, and $R_{ex}(cal)$ are determined as described in section 5.2. Taking $D_w(exit_{std}) = D_{w,ex}(cal)$ and $R(exit_{std}) = R_{ex}(cal)$, the exit dosimetry correction factor, $C_{ex,std}$ is calculated as

$$C_{ex,std} = \frac{\left(\frac{D_w(exit_{std})}{R_{ex}(exit_{std})} \right)}{F_{cal,en}} . \quad (11)$$

6.1.3 Exit SSD correction factors

Measurements to determine the SSD correction factor for photon exit dosimetry, $C_{SSD,ex}$, use the same setup, phantom thickness and diode positioning as for determination of $F_{cal,ex}$ or $C_{ex,std}$ but the SSD is varied over the expected range of treatment distances. The exit and entrance dosimetry SSD correction factors need not be equal.^{62,65,73}

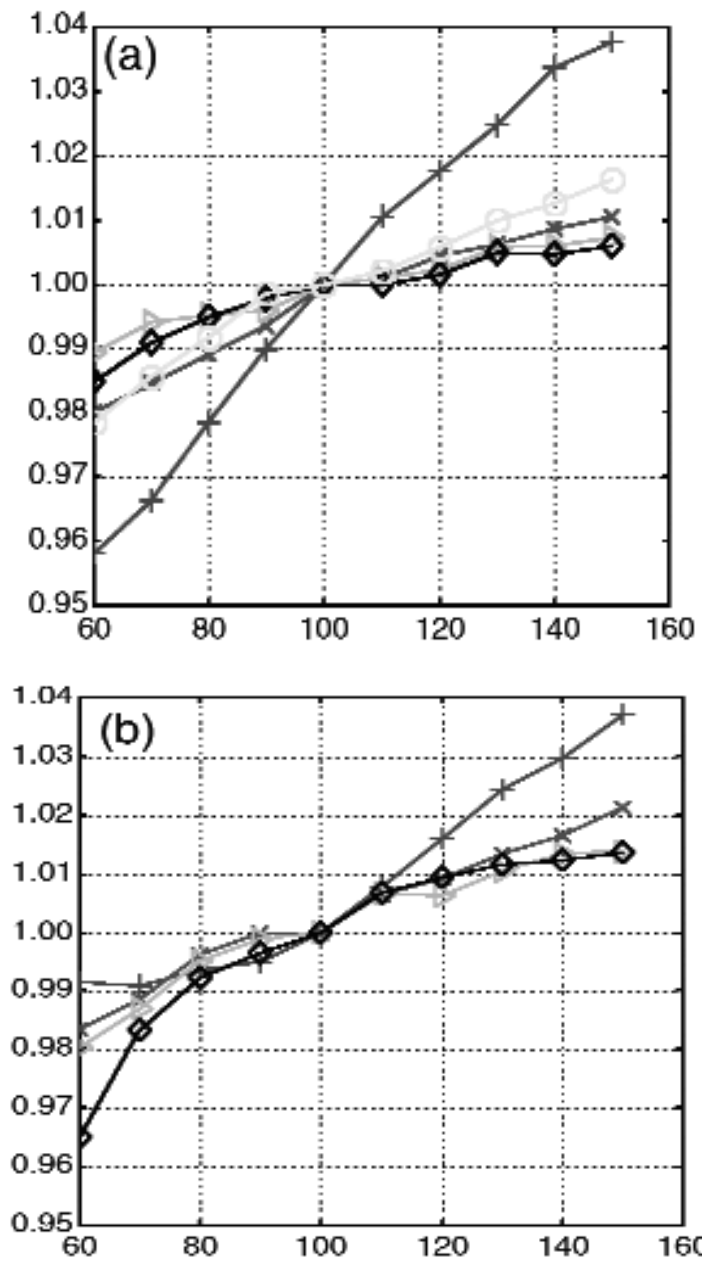


Figure 6. SDD correction factors for diodes measured at the surface in a full scatter phantom under (a) 6MV. (b) 18 MV. + – Isorad Red (n-type), ▷ – Isorad-3 Gold, ‡ – EDP10^{3G}, x – QED Red (n-type), and o – QED Gold (n-type) (cf. references 106 and 109).

6.1.4 Entrance field-size correction factor, C_{FS}

The term “field size” here refers to the irradiated field at the depth of the entrance DDRP. If this is d_{max} , the field-size correction factor, C_{FS} , relates the diode readings to the total scatter factor, $S_{c,p}$.⁵³ Most reports use the same setup for measurements of C_{FS} as for diode entrance dosimetry except that the collimator setting (CS) differs from the calibration setting, CS_{cal} . From equation (7), C_{FS} is given by

$$C_{FS} = \frac{\left(\frac{D_w(CS)}{D_w(CS_{cal})} \right)}{\left(\frac{R(CS)}{R(CS_{cal})} \right)}. \quad (12)$$

If the DDRP depth is at d_{max} , then

$$C_{FS} = \frac{\left(\frac{S_{c,p}(CS)}{S_{c,p}(CS_{cal})} \right)}{\left(\frac{R(CS)}{R(CS_{cal})} \right)}. \quad (13)$$

Equation (13) is exact if the same SSD was used for diode calibration and for measurement of the clinically used $S_{c,p}$ and the approximation is within 1% if the SSD changes within a range of ± 20 cm. Thus $S_{c,p}(CS)$ and $S_{c,p}(CS_{cal})$ can be obtained from the clinical data tables without need of new ion chamber measurements.

Figure 7 is an example of C_{FS} for two diode models in a 6 MV photon beam.⁷⁸ In general, values of C_{FS} reported in literature depend on diode internal construction and buildup materials^{3,5,18,37,51,73,79}, and strong variation of C_{FS} may indicate inadequate intrinsic buildup.^{21,72} While C_{FS} defined above is only strictly valid for unblocked fields, if blocking is not extreme and the equivalent field size at d_{max} is FS , equation (13) is a good approximation for C_{FS} with $S_{c,p}(CS)$ replaced by $S_c(CS)S_p(FS)$. The presence of blocks has little effect^{3,24,81} except for extreme blocking⁶⁵ and/or short SSD.^{37,68} See references 44 and 80 for an unusual approach which accounts for scatter from blocks in both diode response and calculation of expected dose.

For electrons, C_{FS} measurements should include at least the open cones and representative inserts. If the same cone and SSD are used for diode calibration and clinical cone-output factor measurements, the clinical factors can be substi-

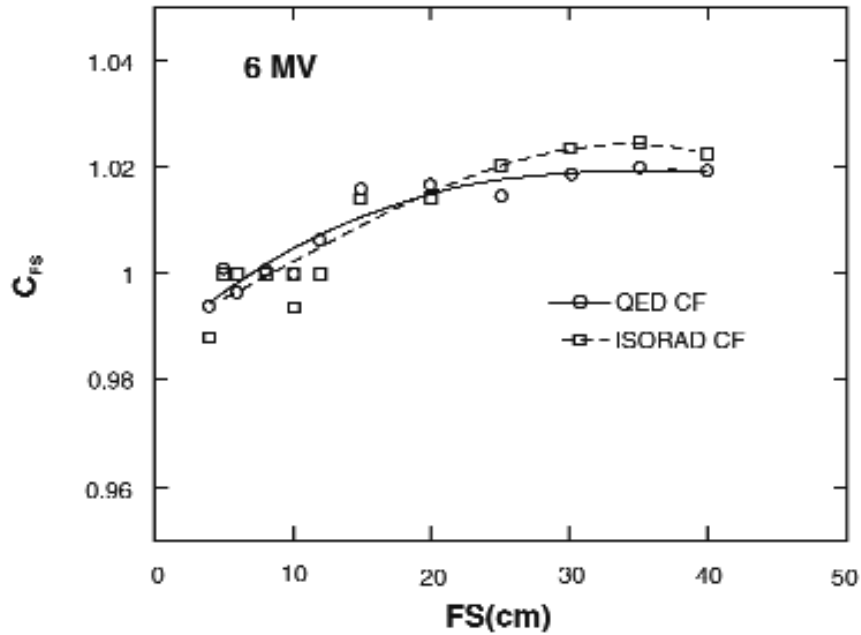


Figure 7. Entrance C_{FS} for two diode models in a 6 MV photon beam (from reference 78).

tuted for new ion chamber measurements. One report⁶⁵ states that a set of electron diodes showed no more than 2% variation from the calibration response for all cones and for energies from 6 MeV to 20 MeV. However, other workers⁶⁶ used a database of measured field-size correction factors in their electron beam in vivo dosimetry program.

6.1.5 Exit field-size correction factor, $C_{FS,ex}$

The setup for photon beam exit dosimetry measurements of the field-size correction factors is the same as for determination of $F_{cal,ex}$ (or $C_{ex,std}$). While equation (12) holds, the replacement of ion chamber measurements by clinical data output factors is not valid. Reports in the literature^{21,65,67} indicate that the exit field size correction factor, $C_{FS,ex}$ is diode and energy dependent. While some report it is almost unity,⁷³ others report ~5% differences at large field sizes.⁶⁵

6.1.6 Entrance accessory correction factor, C_{AC}

The presence of an accessory such as a physical wedge or compensator or a block tray is accounted for by an accessory correction factor. Let AF_0 be the ratio of ion chamber readings per MU at the DDRP in phantom with and with-

out the accessory. Let AF_{diode} be the ratio of diode readings per MU with and without the accessory with the diode on the phantom surface, positioned as for in vivo dosimetry. Although all beam parameters are the same for the measurements of AF_0 and AF_{diode} , these two ratios need not be equal and the accessory correction factor, C_{AC} , corrects for the difference. For a wedge or block tray, AF_0 is the factor at or near the depth of the DDRP. Often, this was measured when the linac was commissioned, and it is sufficient to use the factors from the clinical data tables rather than make new ion chamber measurements. From equation (7), the accessory correction factor, C_{AC} , is given by

$$CF_{\text{AC}} = \frac{AF_0}{AF_{\text{diode}}} . \quad (14)$$

For a given diode and beam energy, each accessory has its own correction factor. Dose per pulse dependence and beam hardening are partially responsible for the accessory correction factors^{37,44,73,78} and contaminant electrons play a role for diodes with insufficient buildup.^{51,60} References on clinical applications of physical wedge correction factors include 3, 37, 44, 65, 77, 78, and 81 and on block tray and blocks.^{37,44,68} No correction factor was reported necessary for a dynamic wedge.²⁴ The task group found no literature on correction factors for internal (universal) wedges (see footnote to section 8).

6.1.6.1 Wedges

Central axis: For wedges on the central axis, AF_0 is the central axis wedge factor available from the clinical data tables. AF_{diode} should be determined from the average of the diode measurements with the wedge inserted in each of its orientations to eliminate effects of small offsets of the wedge center relative to central axis. Diode placement is important; the diode center should be centered at the beam axis, and the long axis of a cylindrical diode should be oriented along the non-wedged direction. Table III demonstrates that the wedge correction factor depends on both the wedge angle and the type of diode.⁷⁸

Off-axis: Off-axis measurements in wedged fields are necessary if in vivo dosimetry is performed when the central axis is blocked or near a field edge (e.g., the tangents in a single-isocenter, three-field breast technique). It is advised that correction factors be determined for several conveniently spaced off-axis points along the wedge direction⁶⁵ so that values at intermediate points can be interpolated. At each point, the numerator of equation (14) is the corresponding off-axis wedge factor from the clinical data tables and the denominator is the ratio of the diode readings with and without the wedge. In general, diode positioning for wedged-field measurements is critical. Off-axis correction factors are particularly important for diodes with a large central axis correction factor such as the 6 MV ISORAD diodes in Table III.

Table III. Examples of central axis wedge correction factors measured on a Varian 2100C for two types of diodes; field size 10×10 cm² (After reference 78).

Wedge	6 MV C_{wedge}		18 MV C_{wedge}	
	QED (p-type)	ISORAD (n-type)	QED (p-type)	ISORAD (n-type)
15°	1.01	1.02	1.01	1.00
30°	1.01	1.03	1.00	1.01
45°	1.02	1.06	1.01	1.04
60°	1.03	1.07	1.01	1.05

A point can be specified by its distance from the central axis at the level of isocenter, and whether it is toward the wedge heel or toe. For in vivo measurements in other planes, a magnification correction back to the isocenter plane determines the off-axis correction factor. For example, if the diode is at 4 cm toward the toe of the wedge and at SSD=80 cm, the correction factor determined at 5 cm toward the toe in the isocenter plane (4/80×100 cm) should be used. A similar approach can be applied to compensator filters,⁴⁴ although for custom compensators individual ion chamber measurements are necessary.

6.1.6.2 Blocking tray

Correction factors for blocking tray (C_{BT}) are reported in the literature.^{5,18,37,44,51,79} The numerator in equation (14) is the tray transmission factor from the clinical data tables. Values of C_{BT} differing from unity are reported⁵¹ especially for diodes with inadequate buildup, where CBT also depends on the diode distance from the tray.^{60,68} There are reports where blocks further affect the diode readings for entrance measurements.^{44,51,68} However, C_{BT} is expected to be close to 1.0 for modern diode detectors with sufficient buildup thickness to remove contaminant electrons.⁵¹

6.1.7 Accessory correction factors for exit dosimetry

Wedge and compensator correction factors for exit dosimetry^{21,65,73} can be measured in a similar fashion to those for entrance dosimetry, but with the diodes positioned as for exit dose calibration. It is particularly important to assure the diode location relative to central axis.

6.2 Intrinsic correction factors

Since intrinsic correction factors are determined only by properties of the diode, their measurement does not involve a change in beam characteristics. In

equations (6) and (7), $D_w(X)$ and $D_w(X_{cal})$ are identical and the equation for an intrinsic correction factor simplifies to

$$K_i = \frac{R(cal)}{R(X)} . \quad (15)$$

6.2.1 Temperature correction factor, K_T

The temperature correction factor at temperature T for a diode calibrated at T_{cal} is defined as

$$K_T = \frac{R(T_{cal})}{R(T)} . \quad (16)$$

The physics behind the diode sensitivity variation with temperature (SVWT) is discussed in section 2.2.3. The temperature coefficient that determines the SVWT is reported to range between $0.6\%/^{\circ}\text{C}$ ^{24,32,37,41,42,73} and $0.3\%/^{\circ}\text{C}$ ⁴³ with lower values characterizing newer-model diodes. Table IV presents measured temperature coefficients for samples of eight currently marketed diodes. The apparent dependence on beam energy is attributed to the difference in instantaneous dose rate between linacs and Co-60.⁴³ The diode sensitivity increases as the temperature increases so that K_T is less than unity when the diode is above the calibration temperature. If a diode is calibrated at therapy-room temperatures ($\approx 20^{\circ}\text{C}$), the dose inferred from *uncorrected* in vivo readings made with the diode equilibrated to patient-skin temperatures ($\approx 28^{\circ}$ to 34°C)⁴⁵ can be over 3% high, even with a state-of-the art diode. The effect of SVWT is reduced if the diodes are calibrated at a higher temperature or if in vivo measurements are made quickly after placing the diode on the patient skin, as it takes 3 to 5 minutes to reach 90% of the equilibrium temperature, depending on diode construction, thermal contact, and room and skin temperature.⁴⁵ At present, at least one commercial system provides automatic temperature compensation.

To measure K_T , the diode is irradiated at several known temperatures. This can be accomplished by taping the diode to a thermally conductive surface in contact with a water bath of variable and measurable temperature.^{45,48,61,70,72} One group⁴³ protected diodes with a thin waterproof sleeve and irradiated them in a water bath. The diode should be in thermal contact long enough to establish thermal equilibrium (time scales of ~ 10 minutes for full equilibrium).^{43,45} It is possible to measure the diode temperature directly by operating it as a thermister.^{44,45}

Table IV. Temperature Coefficients for n-type and p-type diodes. All measurements were made at depth of 5 cm, 10×10 cm², SSD = 100 cm. (TG-62 members AS and TM (private communication) and reference 43)

Diode Type	Type	Temperature Coefficient		
		6 MV (%/°C)	15, 18 or 20 MV (%/°C)	Co-60 (%/°C)
Isorad Gold 1, unirradiated	n-type	0.06	0.05 (20 MV)	0.45 (T1000)
Isorad Gold 2, unirradiated	n-type	0.08	0.10 (20 MV)	0.16 (T1000)
Isorad Red	n-type	0.22	0.21 (20 MV)	0.37 (T1000)
QED unirradiated	p-type	0.27	0.25 (15 MV)	0.34 (T Phoenix)
QED Blue Diode	p-type	0.30	0.31 (15 MV)	0.30 (T780)
QED Gold	n-type	0.63	0.65 (18 MV)	—
QED Red	n-type	0.66	0.62 (18 MV)	—
QED Red Diode	p-type	0.29	0.29 (15 MV)	0.29 (T780)
Scanditronix EDP-10 3G	p-type	0.25	+/-0.1	+/-0.1
Scanditronix EDP-HL 3G	p-type	0.25	+/-0.1	+/-0.1

Accounting for SVWT in vivo is most important for long irradiation times, such as TBI. For short diode-skin contact times, if spot measurements confirm that SVWT is small relative to the accuracy desired from the measurements, temperature correction may be omitted,⁴² or an average K_T based on a temperature increase estimated from temperature measurements on volunteers may be used.⁷¹ Significant variations in K_T have been observed within one batch of the same type of diodes.^{4,37} Thus decisions regarding K_T should be based on in-house measurements rather than generic values of the SVWT.

6.2.2 Angular dependence correction factor, K_θ

The angular dependence of diode response is partly due to the diode buildup configuration and partly due to scatter from the phantom on which the diodes rest. Because both effects cause the response to depend on the incident angle of the beam relative to the diode, it is desirable for vendors to provide data for K_θ that specify the measurement geometry. Most often, clinical K_θ measurements are made with the diode on the surface of a flat phantom. θ is defined as the angle between the beam central axis for the measurement and the beam axis direction during diode calibration (see figure 4). Section 2.3.1 gives a general

discussion of cylindrical and hemispherical diodes. Representative diodes are shown in figure 2 and figure 3, and the geometry of “axial” and “tilt” angular dependences is shown in figure 4. To measure the axial response of a cylindrical diode, the beam axis rotates in the plane perpendicular to the diode axis, while for the tilt response, the beam axis rotates in the plane parallel to the cylinder axis. For axial dependence of hemispherical diodes, the beam axis rotates in the plane perpendicular to the cable; for tilt, the beam axis rotates in the plane of the cable. For hemispherical diodes, axial and tilt directional dependences are approximately equal.

From equation (12), the angular response correction factor is given by

$$K_{\theta} = \frac{R(\theta = 0)}{R(\theta)}. \quad (17)$$

The angular dependences quoted in the literature^{3,19,24,37,60,66} and by vendors are for entrance measurements. In the literature reviewed by TG-62, the angular correction factor for exit dosimetry is set to unity or not mentioned, and no detailed description of its measurements are presented. Figure 8 shows examples of K_{θ} for two diodes with hemispherical/conical symmetry³⁷ in which K_{θ} exceeds 5% for angles above 45°. Cylindrical diodes have weaker axial angular dependence than hemispherical diodes.⁴⁶ The need for angular correction is reduced by positioning the diode so that the beam is as close to normal incidence as possible.

Measurements of K_{θ} for electron dosimetry diodes can be made similarly to those for photon diodes. Literature describes measurements in electron beams incident on a flat phantom,⁶⁶ on a cylindrical phantom,⁴⁹ and in a foam holder.⁵⁶ The latter two methods allow a larger range of gantry angle, but measurements on a flat phantom more closely simulate clinical placements. Because of the effect of obliquity on electron beam dose distributions, clinical electron beams are often at approximately normal incidence and K_{θ} is close enough to unity to be omitted.

Throughout the above discussion, we have neglected the change in dose distribution due to an oblique beam incidence, though this affects the comparison of the diode reading with the treatment plan.

6.3 Patient dependent correction factors: Thickness, C_{thick} , and gap, C_{gap}

Changes in instantaneous dose rate, photon spectrum, and beam scatter may cause exit diode readings for arbitrary patient thicknesses to have a different ratio to the dose at the exit reference depth than for calibration conditions.^{3,34,62,65,73,76}

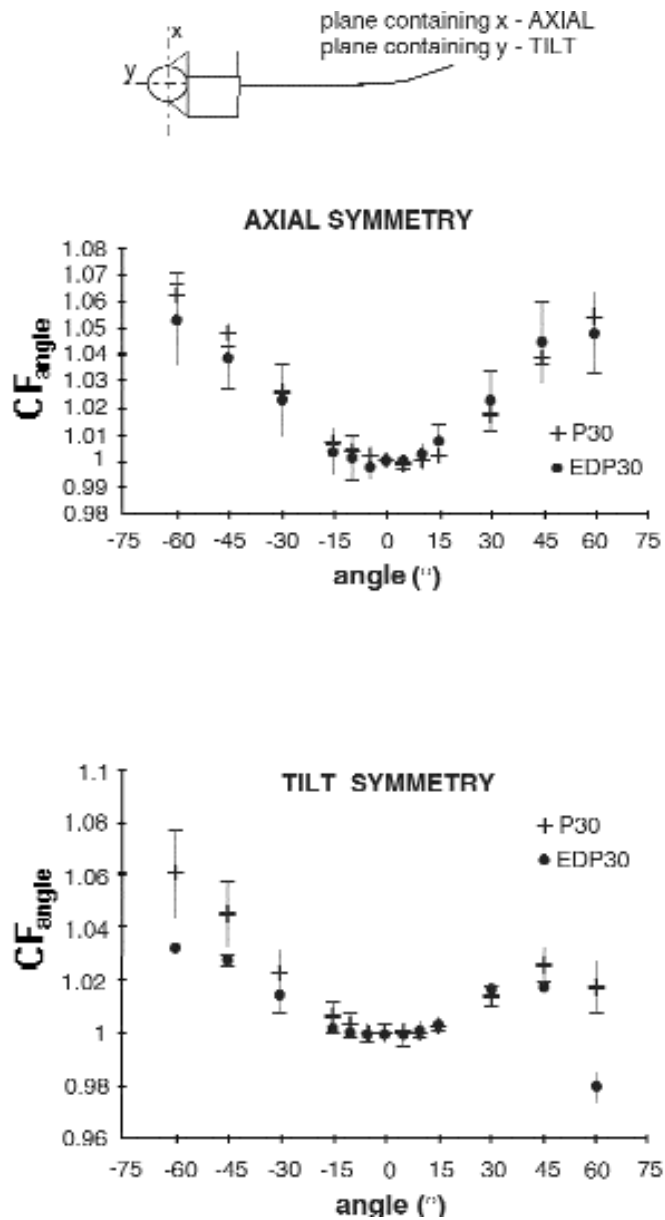


Figure 8. Angular correction factors for two models of diodes; both have hemispherical/conical symmetry (Reprinted with permission from N. Jornet, M. Ribas, T. Eduardo. "In vivo dosimetry: Intercomparison between p-type based and n-type based diodes for the 16-25 MV energy range," *Med Phys* 27:1287–1293. Copyright 2000 American Association of Physicists in Medicine).

Let $D_{w,ex}(t)/MU$ be the dose to water per MU at the exit diode dosimetry reference depth in a phantom of thickness, t , as calculated from the clinical depth dose data. Then, from equation (6),

$$C_{\text{thick}}(t) = \frac{\frac{D_{w,ex}(t)}{MU}}{\frac{D_{w,ex}(t_{\text{cal}})}{MU}} \cdot \frac{R(t_{\text{cal}})}{R(t)} . \quad (18)$$

In the measurements of $R(t_{\text{cal}})$ and $R(t)$, the field size and SSD are the same as for the exit diode dosimetry calibration but the phantom thickness is changed to cover the clinically relevant range.

For entrance measurements for a field incident from below the treatment couch or exit measurements for an AP field, the diode is often taped to the underside of the couch insert so that the patient does not have to lie on it. This produces a gap between the diode and the patient's skin. Further gaps at these and other beam angles are introduced by immobilizing molds.⁸¹ Gaps cause changes in both source to diode distance and scattering conditions relative to the calibration conditions on a solid phantom surface. A gap correction factor or combined thickness and gap correction factors for exit dosimetry may be measured by simulating these situations with a range of mold and phantom thicknesses.^{4,21,68,70,83}

7 CONTINUING QUALITY ASSURANCE OF A DIODE IN VIVO DOSIMETRY SYSTEM

Continuing QA is a necessary component of a diode-based in vivo dosimetry program. Table V is a sample QA schedule. The rationale for the suggested frequency of tests is described below, but devising a QA schedule to meet the needs of an individual practice is the responsibility of the clinical physicist.

Daily/Weekly: The mechanical integrity of the detectors and system cabling is a constant concern. Therapists should be encouraged to report deterioration and a documented visual inspection of the diodes in the room and their cabling should be part of the weekly linac QA.

Weekly, semi-weekly, or monthly: The frequency of these tests should be determined by the dose received by the diodes and their expected sensitivity variation with accumulated dose (SVWAD).^{4,15,21,31,37,41,42,44,47,48} In general, caution is advised for new users and new diodes. SVWAD, which is discussed in section 2.2, is associated with changes in diode sensitivity and dose-per-pulse and temperature coefficient^{42,44} and consequent changes in calibration factor, C_{SSD} , C_{wedge} and K_T . SVWAD is worse for diodes used in electron or higher photon

Table V. Sample QA Schedule for an established diode system in frequent use.

Frequency	Procedure	Tolerance
Daily or weekly	Visual inspection System cabling Mechanical integrity of diode	functional functional
Weekly, biweekly, or monthly	Confirm/reestablish diode calibration factor based on monthly linear accelerator calibration Spot check CF_{SSD}	<2% change <2% change
Annually	Drift, linearity, confirm/reestablish diode calibration factor based on monthly linear accelerator calibration Check all correction factors	Drift, linearity as at acceptance, calibration change <2% <2% change
Battery replacement	Check calibration factor same as monthly QA	<2% change

energy beams^{16,31,33,46,84,85} and for old-model diodes.¹⁶ For current generation diodes, vendors quote SVWAD in photon beams <15 MV at <1% per 250 Gy (one vendor quotes <0.1% per kGy at 6 MV and <2% per 250 Gy at higher energies). The expected rate of sensitivity change with clinical use has implications for the frequency of diode calibration.⁴⁸ The weekly accumulated dose can be estimated according to clinical use (one diode used for entrance dosimetry of 5 new patients/wk at 2 Gy/treatment acquires approximately 10 Gy/wk). Users who suspect high SVWAD and/or have a busy in vivo dosimetry program may wish to check calibration factors weekly or semi-weekly⁶⁰ while those with low usage and/or known low SVWAD find monthly tests sufficient.

Even if the characteristics of a matched set of diodes are the same at commissioning, SVWAD can lead to changes over time depending on each diode's radiation history. At least a monthly check of calibration factors for a new system or a new diode is advised for the first 2 to 3 months of use. It is also advisable to spot-check C_{SSD} by comparing the diode response at a short SSD relative to the calibration SSD (e.g., 80 cm vs. 100 cm). Significant change in C_{SSD} ($\geq 2\%$) from the commissioning value warrants measurement of a new set of SSD correction factors if they are used clinically or implementing them if they are not. It is advisable to replace a diode for which the SSD correction becomes too large (>10%).

Annually: TG-62 advises annual QA system tests including repeats of the post-irradiation signal drift and linearity tests performed at acceptance (see

section 4) and checks of the calibration factor(s) and the correction factors in clinical use. Factors which have changed by more than a user-selected amount (e.g., 2%) from the values established during commissioning or the previous annual QA should be updated.

Special attention should be paid to C_{SSD} , C_{wedge} , and K_T that are known to change with total accumulated dose. Even if these factors were not used during the past year, one or more of them may have become sufficiently different from unity to affect the level of in vivo dosimetry accuracy. It is the physicist's responsibility to demonstrate that the need for the correction factors has not changed over the course of the year.

A useful annual QA test is to perform a phantom simulation of one or more common treatment scenarios with either a slab or anatomical phantom. By comparing the diode measurements with calculations and ion chamber or film measurements, the integrity of the entire in vivo dosimetry chain from dose calculation through diode dosimetry is confirmed.

Special circumstances: Diode calibration should be checked when the electrometer battery is changed, or if there are substantial machine alterations affecting the beam output or energies, new collimators, wedges, or electron cones. Physicists who identify other conditions in their individual practice that require more frequent QA checks should design a schedule they deem suitable.

8 CALCULATING EXPECTED DOSES FOR DIODE IN VIVO DOSIMETRY

Both diode and TLD in vivo dosimetry place a dosimeter on the patient's skin and compare its reading with a value calculated from the planned dose distribution in the patient. Therefore, methods that were developed to compare calculated doses with TLD in vivo measurements also apply to diode dosimetry and are referenced in this task group report.^{5,14, 69}

In diode entrance dosimetry, equation (9) converts the diode reading, R , to D_{diode} , the inferred dose at the diode dosimetry reference depth along the ray through the diode. Let D_{calc} be the calculated dose delivered to some chosen checkpoint by the planned beam, as calculated with clinical beam data tables and/or the treatment planning system. There are three equivalent strategies described below to compare D_{calc} with D_{diode} .

1. Choose the checkpoint at the depth of the DDRP (e.g., d_{max} below the diode). Then each beam has a different checkpoint. Back-calculate D_{calc} from the planned dose delivered by each beam to a point that is significant relative to the treatment plan, such as the ICRU prescription point.⁸⁶ Use equation (9) to convert R to D_{diode} and compare D_{calc} with D_{diode} .^{3,20,70} This method is particularly convenient if the diode dosimetry system out-

put incorporates calibration and correction factors and presents the diode reading directly as D_{diode} . If D_{calc} for each beam is provided in a paper or electronic worksheet, the therapist can easily detect problems “on the fly.” Alternatively, the product of the calibration and correction factors can be tabulated in the worksheet, and the therapist can calculate D_{diode} from the diode reading.

2. Choose a checkpoint, P , which is directly related to the planned dose distribution such as the ICRU prescription point. In this case, all the beams in the treatment plan have the same checkpoint. D_{calc} is known from the treatment plan and/or the prescription. Calculate D_{diode} from R [equation (9)] and use the clinical beam data tables and/or isodose distribution to calculate the inferred dose at P , $D_{\text{diode}, P}$, from D_{diode} . Compare $D_{\text{diode}, P}$ with the planned dose at P .^{4,19}
3. Choose the checkpoint according to either method (1) or (2) and use the treatment plan isodose distribution and/or clinical beam data tables to calculate the D_{diode} for each beam. Then calculate the expected diode reading, R_{calc} , by inverting equation (9) to get

$$R_{\text{calc}} = \frac{D_{\text{calc}}}{F_{\text{cal, cn}} \prod_i K_i \prod_j C_j}, \quad (19)$$

and compare it with the measured diode reading R . This method is quickly interpreted by a therapist if R_{calc} is provided for each field in a worksheet.

These three methods give equivalent information. Which one is used depends on personal preference and clinical logistics.*

Two different approaches to calculating the expected dose, D_{calc} , are described in the literature. These are:

1. Use the prescribed dose to calculate D_{calc} from clinical data tables or with the treatment planning computer. This method is used by almost all the clinical applications referenced in this report.
2. Use the monitor units (MU) in the patient’s chart for each beam together with the clinical beam data tables to calculate D_{calc} .^{44,79}

*A task group member (TZ) uses method 3 for in vivo dosimetry of treatments where a fraction f of the calculated dose D_{calc} is delivered with a universal wedge and $(1 - f)$ is delivered with open field. If CF_w is the wedge correction factor for a completely wedged field ($f = 1$) then

$$R_{\text{calc}} = \left(\frac{f}{CF_w} + (1 - f) \right) \frac{D_{\text{calc}}}{F_{\text{cal, cn}} \times \text{product of all other correction factors}}$$

These approaches are *not* equivalent, although both can detect many treatment errors, including incorrect wedge, SSD incorrect by more than 2 to 3 cm, or delivered MU different from planned MU.

TG-62 favors approach 1 but recognizes that there are differences in clinical practice and that both methods are established in the literature. Approach 1 requires less input data than approach 2; specifically, knowledge of the planned dose delivered by the beam of interest (the prescribed dose and beam weight for each field) and TMR or PDD data tables, but it is independent of wedge, tray, and output factors. It is directly related to the physician's prescription, the fundamental quantity to be confirmed.

Approach 2 starts from the already-calculated MU and reuses the beam data parameters from which the MU were calculated in the first place, including treatment accessory factors. The measured dose and expected doses calculated according to approach 2 can agree even when the MU would deliver the wrong dose to the prescription point. For example, using approach 2 in the presence of a dose doubling error, the dose which is back-calculated from the incorrect MU will agree with the measured dose, though it is twice as large as prescribed. Although the pre-treatment chart check *should* have picked up such an error, serious errors of this sort occasionally are missed by the chart checker, and an important function of in vivo dosimetry is to catch them further downstream in the QA process. If a chart check already missed this error, approach 2 risks missing it again, especially if the in vivo dosimetry reviewer looks only at agreement between in vivo measurements and calculation.

For entrance dosimetry, the calculation of D_{calc} , either manually or from the treatment planning system, is straightforward.^{5,53,74} Detailed discussion of methods for efficiently combining inferred doses from entrance and exit dosimetry to obtain the total dose at a chosen point in the patient is beyond the scope of this report, and readers are referred to the literature.^{5,14(Ch 1),19,69,76,87,88}

9 POSITIONING CONSIDERATIONS

Incorrect diode placement is a frequent cause of diode readings that trigger clinical investigation because they exceed action levels.^{6,20,34,62,66,70,81} To accurately and efficiently use diodes for in vivo dosimetry, correct placement is crucial. Except for deliberate gaps (see section 6.3.1), there should be secure contact between the patient's skin and the diode, with a cylindrical diode in contact over its entire length and the flat side of a hemispherical diode against the patient's skin (c.f. sections 5.1.3, 5.2.2, and 6.3.1). The ray through the diode center should pass through a point where the dose can both be accurately calculated and back-calculated to the diode dosimetry reference depth. The placement point should be documented and reproducible for follow-up measurements. The central axis is a reproducible location, but if it is closer than 1 to 2 cm to a field edge, a preferable diode position is near the center of the irradiated field where the dose gradient is small.⁴

A diode in an electron field strongly perturbs the dose distribution.^{1,48,49,55,66} This is graphically demonstrated in figure 9, a film at d_{\max} of a 9 MeV electron beam, defined only by 20×20 cm jaws. Three different diodes, each intended for electron dosimetry, are on the phantom surface at corners of a 3 cm square. Each diode reduces the dose by at least 15% over an ~1 cm diameter region. To minimize the shadowing effect, if several measurements are made during a treatment course, the diode location should be changed between fractions. Because the dose reduction particularly perturbs the dose distribution in a small electron field, in vivo dosimetry in electron fields of 1 to 2 cm diameter may be better performed with TLD, and if a diode measurement is necessary, the effect of the dose perturbation should be carefully considered.

Precise positioning is particularly important in wedged fields, and it is important that the therapists understand the need for placement precision on the order of a few millimeters for wedged field measurements. At the level of isocenter, a 1 cm displacement along the wedge gradient for a 45° or 60° wedge causes an approximate 3% to 6% dose change. Cases involving combinations of wedges and obliquely incident beams are especially problematic.⁸¹ The axis of a cylindrical diode should be perpendicular to the wedge gradient to minimize uncertainties. Diode positioning for exit measurements requires particular care because it is difficult to discern the diode location relative to aperture edges or a wedge profile. When entrance and exit diodes are placed simultaneously, they should be slightly offset to avoid shadowing effects. Portal imaging is advantageous in verifying the exit diode placement and for determining the presence of tissue inhomogeneities such as bowel gas, lung, femoral heads, or high-density implants within the field.^{4,21,65,87,89} Positioning problems and tissue inhomogeneities lead to greater uncertainties during exit dose measurements.^{3,7,34,62,79}

10 OTHER IN VIVO MEASUREMENT APPLICATIONS OF DIODES AT STANDARD TREATMENT DISTANCES

Below, TG-62 discusses in vivo dosimetry applications of clinical interest for which there is little peer-reviewed information regarding diodes. TG-62 recommends great caution in such clinical applications pending further study.

10.1 Out-of-field and skin doses

In vivo dosimetry is often used to estimate doses to normal structures outside of the treatment fields such as eye lens, pacemakers,⁹⁰ fetal dose,⁹¹ and testicular dose.⁹² While measurements of low out-of-field doses may not require great relative accuracy, many physicists strongly prefer to use TLD¹ to minimize uncertainty due to photon energy, dose-rate, and angular dependence. A comprehensive comparison of diodes to TLD or ion chambers for in vivo measurement of out-of-field doses has not, to our knowledge, been published. However,

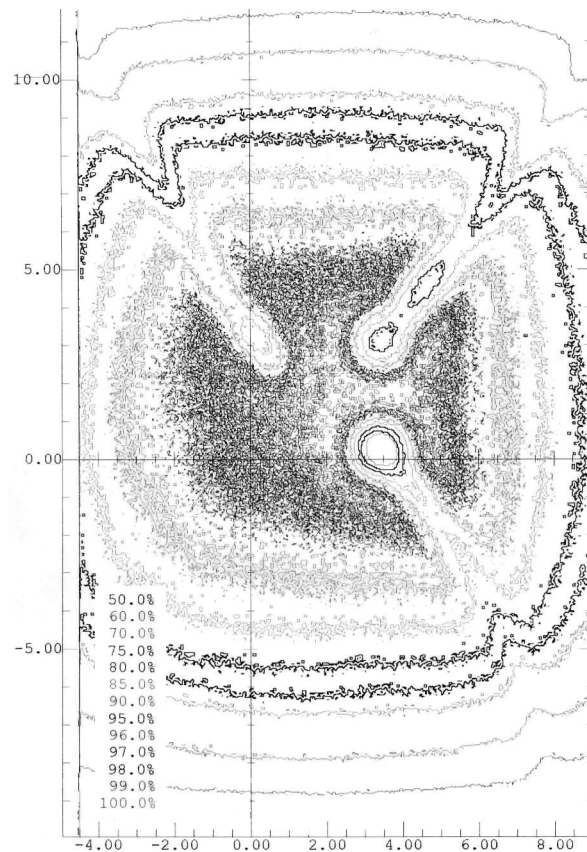


Figure 9. Film at the d_{\max} of a 9 MeV electron beam with three diodes placed on the surface of the phantom. The diodes are at three corners of a 3 cm square centered on central axis. The beam is defined by a 20×20 cm collimator only (no cone). In clockwise order from the upper left corner, the diodes are Scanditronix EDD2, Sun Nuclear QED 111200-0, and PTW L991065. The dose was normalized to the fourth corner of the square⁴⁹.

out-of-field measurements made in phantom with a commercial diode array agree well with ion chamber⁹³ measurements. One publication⁶⁷ reports measurements of contralateral breast doses using diodes rated for 6 to 12 MV and calibrated for out-of-field measurements by comparing ion chamber measurements at 1.5 cm depth in phantom and diode measurements for a range of distances from the field edge. Scanditronix Wellhöfer provides diodes with minimal buildup and small angular dependence for “risk organ monitoring” and advises a similar methodology to relate the diode reading to out-of-field ion

chamber measurements, and Sun Nuclear provides a diode with no buildup (stated 0.11 g/cm²) for skin dose measurement (see table I).

10.2 Intensity-modulated radiation therapy (IMRT)

Early in the development of sliding window and step-and-shoot intensity-modulated radiation therapy (IMRT), TLD were used for monitoring treatments,^{94,95} and there is a recent study⁹⁶ of diode in vivo dosimetry for such IMRT treatments. The ability of diodes to accurately measure dynamic intensity modulated fields is not an issue, as demonstrated by the success of linear diode arrays for phantom measurements in dynamic wedge fields,⁹³ and two-dimensional arrays for dosimetric QA of IMRT fields.^{97,98} Diode in vivo dosimetry in dynamic wedge fields is also reported.^{24,107} However, the reliability of any point in vivo measurements done in the high gradient setting of IMRT is subject to question.^{97,105} Nonetheless, it may be argued that if in vivo point dose measurements are compared with phantom measurements from the same intensity distribution, some very serious delivery errors can be apprehended, including treatment with a file intended only for port films or the programming of the incorrect dose per fraction for treatment.

10.3 Kilovoltage therapy

Measurements evaluating the low-buildup skin dose monitoring diode mentioned above for in vivo dosimetry in beams ranging from 20 to 100 kVp indicate that, with further study, such use may be possible.⁵⁰

11 DIODE IN VIVO DOSIMETRY FOR TOTAL BODY IRRADIATION (TBI)

11.1 Rationale for in vivo dosimetry for TBI

TBI treatments administer potentially lethal doses in a small number of treatments often using very extended SSD (>300 cm), low dose-rate, nonstandard patient positions, and a variety of treatment aids such as beam spoilers or partial-transmission lung blocks. Although parallel opposed beams are used (APPA or opposed laterals) the patient must be turned between beams. Some protocols mandate a documented level of midplane dose uniformity over the patient's body, requiring compensation for missing tissue and lung inhomogeneity. For these reasons, in vivo dosimetry is strongly recommended⁹⁹ and is required by some protocols. While ion chambers, TLD and diodes have been used, the ability to obtain real-time output at multiple anatomical sites with a durable dosimeter makes diodes particularly well suited to TBI in vivo dosimetry. Diodes have been used alone or in combination with portal films.⁸⁹ Special requirements for diode systems intended for TBI measurements are listed in section 3.2.

11.2 Acceptance, calibration, and correction factors for TBI

Because the TBI irradiation conditions are very different from those for conventional treatments, acceptance testing and calibration of the diodes should be performed under these conditions. The considerations discussed in section 4 regarding linac dose linearity and dose calibration, diode placement on the phantom surface, individual diode calibration factors, and written documentation apply to these measurements. The system's electronics, including cables connecting to the readout at the console, should be kept out of the direct beam to prevent radiation damage and spurious readings and to minimize the stem effect. Recently, systems without cables have become available.

11.2.1 Acceptance measurements

1. *Post irradiation signal drift:* This test can be performed at a conventional treatment distance, a simpler setup requiring fewer MU. Because TBI irradiation times are long, the drift tolerances need to be stricter than for conventional distance treatments. At approximately 100 cm SSD, irradiate the diodes with 100 MU and note the display reading immediately after the beam goes off. Keep the unit in measurement mode and note the change in display. After 5 minutes, the change in display should be <0.5%.

For tests 2 and 3, securely fasten the diodes to the entrance surface of a plastic phantom near central axis at the extended distance and large collimator setting that are used for TBI.

2. *Short-term reproducibility:* Deliver between three and five exposures with MU calculated to give a dose of 1 Gy at d_{\max} at the TBI location. Run the accelerator at the dose-rate (MU/min) appropriate to your TBI treatments. Record the readings of each diode for each exposure. If, after three exposures, the ratio of maximum to minimum reading for a diode exceeds 1.04, perform two more irradiations. If the ratio of maximum to minimum diode readings in the last four exposures is ≤ 1.04 , accept the last four readings as accelerator drift during the first irradiation may have caused the first reading to be an outlier.
3. *Dose linearity:* Immediately after the short-term reproducibility test, check dose linearity under TBI conditions. Make five exposures using MU calculated to give a dose at d_{\max} of 0.2 Gy and average the readings to obtain Average (Min MU). Similarly, make five exposures at the MU which would give a d_{\max} dose approximately 10% higher than the maximum expected for TBI in your practice. Average these to obtain Average (Max MU). The following ratio should be between 0.98 and 1.02:

$$\frac{\text{Average (Max MU)}}{\text{Average (Min MU)}} \div \frac{\text{Max MU}}{\text{Min MU}}$$

Failure to meet these criteria may be due to excessive leakage current. Especially if this is a new in vivo dosimetry system, consult with the vendor.

11.2.2 Entrance dose calibration

It is assumed that TBI relative dosimetry measurements including TMR and beam spoiler transmission have already been performed.⁹⁹ Thus, the ratio, r_{TBI} , between $D_{\text{w},0}/\text{MU}$, the dose/MU to water under TG-51 reference conditions, and $D_{\text{w},\text{TBI},0}/\text{MU}$, the dose/MU to water at the TBI entrance DDRP for the TBI in vivo dosimetry reference conditions can be calculated from the standard distance and TBI clinical data tables. The TBI reference conditions include the SSD, accelerator dose rate, collimator setting, and beam spoiler, if that is commonly used. To calibrate the diodes for TBI in vivo dosimetry under the TBI reference conditions, first check the accelerator output constancy with the TG-40 monthly check procedure at conventional distance (see section 5.1.2). Use the same MU/min setting as for TBI. Then calculate the dose to water per MU under TBI reference conditions from

$$\frac{D_{\text{w},\text{TBI},0}}{\text{MU}} = \frac{r_{\text{TBI}} \cdot D_{\text{w},0}}{\text{MU}} . \quad (20)$$

As with calibration at conventional SSD (see section 5.1.2), the diode calibration is slaved to the results of the accelerator output constancy check.

The same phantom can be used for TBI and conventional SSD diode calibration. To establish the entrance calibration factor, $F_{\text{cal.en,TBI}}$, the diode(s) are secured flat against the surface, near the central axis on the entrance surface of the phantom. For in vivo use, the temperature correction to the diode reading may be significant because of long TBI irradiation times. For diode systems without automatic temperature compensation, the user may raise the phantom or the room temperature and perform the TBI calibration at approximate skin temperature (~ 31 °C). At minimum, the phantom temperature at calibration should be recorded and the diodes should be on the phantom long enough (5 to 10 minutes) before irradiation to reach thermal equilibrium.

If the diode reading for irradiation with M MU is $R_{\text{cal.en,TBI}}$, then its TBI entrance calibration factor is

$$F_{\text{cal.en,TBI}} = \frac{\left(\frac{M \cdot r_{\text{TBI}} \cdot D_{\text{w},0}}{\text{MU}} \right)}{R_{\text{cal.en,TBI}}} . \quad (21)$$

Some institutions perform TBI for small children and/or partial-body irradiations at a shorter distance, which is nonetheless far from isocenter (e.g., at floor level beneath gantry). A separate diode calibration is advised for such situations.

Some protocols shield the lung with partial transmission blocks during TBI and then boost the chest wall with electrons with the patient on the treatment couch at a conventional SSD. In vivo dosimetry for these electron fields is handled by electron-beam entrance dosimetry at conventional distance (see sections 5 and 6).

11.2.3 Exit dose calibration

If diodes will also be used to monitor exit doses, either an exit dose calibration factor or an exit dose correction factor should be measured^{22,72,100} under typical TBI conditions (field size, beam spoiler, etc.) and a representative phantom thickness, t , and with the entrance surface of the phantom at the TBI SSD. $D_{w,ex,TBI}/MU$, the dose per MU to water at the TBI exit DDRP (usually on the central axis at depth = d_{max} upstream of the exit surface), is calculated from equation (20) and the TBI relative dosimetry data tables. The diodes are fastened to the phantom exit surface, oriented as for exit dose calibration at conventional distances (cf. section 5.2.3), and the phantom temperature is recorded. If the diode reading for M monitor units is $R_{cal,ex,TBI}$, the exit calibration factor is

$$F_{cal,ex,TBI} = M \left[\frac{D_{w,ex,TBI}}{MU} \right] \frac{1}{R_{cal,ex,TBI}}. \quad (22)$$

Alternatively, the exit diode measurements can be related to the dose at the exit dosimetry reference point through a correction factor (cf. section 6.1.2).

11.2.4 Correction factors

The SSD correction factor is close to unity because at typical TBI distances of 300 to 500 cm, distance changes of 1 to 10 cm cause negligible relative change in instantaneous dose rate, electron contamination, or inverse square. Therefore, most users omit $C_{SSD,TBI}$ for TBI in vivo dosimetry. If a single collimator setting is used for all TBI irradiations, no field-size correction factor is required. Finally, with careful diode placement, the TBI fields are incident approximately normally, eliminating the need for angular correction.

Reports differ on the need for a correction factor to account for patient thickness at exit dose measurement sites.^{20,22,72,73} This should be assessed by individual users for their own measurement systems and programs. Particular caution

is needed in interpreting exit measurements when the rays reaching the diode cross tissue inhomogeneities such as dense bone or lung.

Temperature correction may be significant under TBI conditions, where the diodes are in contact with the patient for up to an hour. The need for temperature correction can be evaluated by calculating average correction factor based on temperature measurements on volunteers or the skin of TBI patients,²³ and the diode temperature during treatment can be similarly determined. Possible diode cooling should be considered if patient repositioning requires lengthy diode removal and temperature correction is being used. Under such circumstances, an additional few minutes of renewed skin contact before irradiation should be allowed for re-equilibration.

Need for an accessory correction factor should be assessed if diodes are used to determine the dose under partial transmission lung-shielding blocks, which change both instantaneous dose rate and beam quality.^{72,101}

11.3 Phantom measurements to establish action levels

The choice of action levels is important for TBI because of the potentially lethal doses that are delivered over a small number of fractions. Reasonable levels are a compromise between treatment accuracy and logistic nightmare. For the entrance dose at the prescription point, $\pm 5\%$ is considered a reasonable level. At off-axis locations, for exit dosimetry and for combined entrance and exit dosimetry to assess dose homogeneity, measurements in a slab and/or anthropomorphic phantom are strongly advised to help determine a realistic action level.^{22,72,100,101} If a TBI program has previously used TLD, it is useful to compare phantom and then patient measurements with the two types of dosimeters for a few (5 to 10 patients) before switching completely to diodes.¹⁰⁰

11.4 Continuing QA

The periodic QA schedule is based on the frequency of diode use and on their estimated SVWAD (see section 7). For a common TBI schedule of 2 Gy fractions, twice daily to 12 Gy, with in vivo dosimetry at each treatment, a diode receives approximately 12 Gy per patient so that a single TBI patient is equivalent to 6 conventional treatment “new starts.” TBI may be infrequent (sometimes less than 1 or 2 per month), but some institutions use the same diodes for all treatments on a single linac. The physicist is advised to weigh these considerations and devise a continuing QA schedule based on estimated accumulated dose as well as time.

Table VI is a sample of a schedule for an established diode system which is used only for TBI in vivo dosimetry.

Although diode systems that are designed for TBI are not expected to require more frequent recalibration, a recent publication⁵⁷ reports on a system that had signal degradation equivalent to 5% for 50 Gy over its first 2 months of use,

Table VI. Sample QA schedule for an established diode system used only for TBI in a clinical practice with at least one patient per month.

Frequency	Procedure	Tolerance
Before each use	Visual inspection System cabling Mechanical integrity of diode	Functional Functional
Before each new patient for a new system—then, if >2–3 patients/month and stable system, weekly, semiweekly or monthly (reference 72)	Confirm constancy of diode calibration factor	<2%
Annually	Drift, linearity, reestablish diode calibration factor based on linear accelerator calibration Check all correction factors	Drift, linearity as at acceptance, calibration factor change <2% <2%
Battery replacement	Confirm calibration factor	<2%

unlike systems from the same vendor used at conventional distances. The user should check diode calibration factors before each new TBI patient during the first 2 to 3 months (or 5 to 10 patients) of clinical operation and discuss unexpected sensitivity changes with the vendor. Diodes used to monitor TBI are often subject to more mechanical stress than those used at standard treatment distance, which makes careful visual inspection of the diodes and cables before each application important QA.

11.5 Comparison of diode readings and expected patient doses

To avoid problems in comparison of diode readings and expected doses, it is important that the diodes be well secured to the patient so that they do not move unintentionally during the lengthy irradiation. Diode positions should be rechecked after the patient is moved to irradiate the other side.

11.5.1 Single-point entrance dosimetry

The methods described in section 8 for comparing dose inferred from diode reading to calculated dose in patient also apply to TBI. Calculations of the expected dose at the TBI entrance dosimetry reference depth are made using

the TBI beam data tables.⁹⁹ The single-point entrance in vivo measurement is usually made at the anatomical level of the prescription point (often the umbilicus or mid-pelvis).²² This requires either two diodes or repositioning a single diode when the patient is rotated. Entrance dosimetry verifies that the patient is at or close (within ~10 cm for a 5% tolerance at TBI distances) to the intended SSD and that the MU are approximately correct. This guards against dose doubling or halving and is also valuable on accelerators where each field must be broken into several MU segments, each below a machine-determined maximum (often $MU \leq 999$). For institutions with several TBI dose-fractionation protocols, it verifies that the correct protocol is being applied. The real-time readout capabilities of diode systems are best exploited if the therapist is provided with a patient-specific worksheet specifying the acceptable range of raw diode readings for each TBI beam. The worksheet should be independently checked as part of the pre-treatment chart check, updated at each irradiation session, and reviewed by a designated individual before the patient's next treatment.

If the readings fall outside the action level, TG-62 advises that the therapists inspect the setup, particularly patient location, diode placement, and cables. Incorrect setup SSD should be handled according to clinical practice for treatment delivery errors. If no diode placement problem is detected, a designated member of the physics staff should promptly inspect the setup, review the monitor unit calculations, and advise on further actions. There are protocols that call for a single-fraction TBI to deliver a total body dose of 1 Gy or more. For these, it is advisable to deliver part (e.g., 25%) of the dose from a field and compare the in vivo readings with the relevant calculations before completing irradiation with that beam. It is advisable for a physicist to be easily reachable when a single fraction TBI is in progress.

11.5.2 In vivo dosimetry to document dose homogeneity

More complex TBI in vivo dosimetry programs combine entrance and exit in vivo measurements from which the midline dose is inferred at several anatomical sites to assess dose homogeneity^{22,23,72,100,101} and the adequacy of missing tissue and lung compensation. This requires a set of diodes, all calibrated under TBI conditions. In vivo dosimetry to assess dose homogeneity should supplement, not replace, the single-point entrance measurements described in section 11.5.1.

An entrance and exit pair of diodes at each site, placed so they do not shadow each other, provide the most complete information. However, it is common to use a single diode at each site to measure the entrance dose from one field and the exit dose from the opposed field. In either case, diode positions should be checked after the patient is moved between fields. If a diode is used for both entrance and exit measurements, it needs both calibration factors or an exit correction factor.

It is helpful to clearly and permanently mark each diode so that the therapist can rapidly document its placement. Color-coding with durable tape is one

means of identification. Some clinics place the same color at the same anatomical site for each irradiation (e.g., blue=head, green=mid-pelvis). The therapist records diode placement and the readings after each beam is delivered on a patient-specific worksheet. For some systems, the printed output identifies individual diodes and substitutes for a worksheet. It is generally useful to keep a separate record of each entrance and exit reading, which are later converted to entrance, exit, and midline doses using the associated calibration factors; any correction factors considered necessary; and one of the several approaches to calculating the midline dose described in the literature.^{14,22,23,73,88,101} TG-62 strongly advises that the methodology for both measurements and calculations be checked in phantom before clinical application.

The action levels for acceptable dose uniformity depend on the TBI protocol and the judgment of the physician and physicist. To exploit the diode system's real-time readouts, the dose homogeneity measurements should be checked by a designated reviewer before the patient's next treatment session to allow for timely corrections. Entrance dose measurements at the prescription point are often required at each treatment to verify the magnitude of the dose delivered. However, if the midplane dose uniformity is determined to be adequate after 1 to 2 treatments and if it is permitted by the treatment protocol and/or institutional policy, multiple-point measurements may be discontinued for the remaining treatments. It is important to be aware that tissue inhomogeneities, which are seldom accounted for in calculating midline doses for TBI, affect the exit diode readings.^{22,23,101} An interesting combination of diode dosimetry and portal films to assess dose homogeneity in TBI is described in reference 88.

12 IN VIVO DIODE DOSIMETRY FOR TOTAL SKIN ELECTRON THERAPY (TSET)

Total skin electron therapy (TSET) treats superficial lesions covering a large area of the body.^{53,82,102,103} The goal is to deliver dose uniformly to the entire surface region. Multi-point in vivo dosimetry may be performed to determine how closely that goal is met. For a common U.S. technique, the patient assumes six different positions in a TSET stand at very extended distance (300 to 500 cm) and, in each position, is irradiated by a pair of obliquely angled 6 or 9 MeV electron beams with only jaw collimation.¹⁰³ Other techniques are described in the literature.⁵³ Since the depth of maximum dose for a TSET beam is usually at the surface, an electron diode with minimal buildup should be used for TSET in vivo dosimetry.

12.1 Calibration of diodes for TSET

Because scattering in air reduces the mean energy of a 6 MeV electron beam to 1.5 to 2.5 MeV at the patient surface depending on the SSD, the diodes must be calibrated at the TSET treatment distance and field size. The calibration can

be done using a single horizontal field. After the surface dose/MU (D/MU) at the center of the field is determined using a calibrated parallel-plate ionization chamber^{82,102,103}, the diodes should be fastened to the entrance surface of a slab phantom (cf. section 5.1.1) at the center of the field and irradiated with M MU, resulting in a reading R . The diode calibration factor is

$$F_{\text{cal, TSE}} = M \left[\frac{\frac{D}{\text{MU}}}{R} \right]. \quad (23)$$

12.2 Special requirements of TSET diode in vivo dosimetry systems

Any electron diode with weak directional dependence can be used. A multi-channel electrometer which can handle multiple diodes is desirable. Although the in-room electrometer case is expected to be sufficiently thick to shield the electronics against electron irradiation, it should be outside the direct electron field if possible. The stem effect for irradiation of the BNC cable connecting the system to the readout at the console should be checked, although this effect is usually negligible.

The TSET dose rate is very low—a typical value of (D/MU) is between 0.04 and 0.05 cGy/MU. The whole treatment session may last 20 to 30 minutes, including time to set up the patient in each new position, and the cumulative diode reading from multiple fields is used during monitoring. Therefore, it is important to ensure that the leakage current is small or that it is properly subtracted by the in vivo dosimetry system using tests similar to those suggested for TBI (section 11.2.1).

12.3 Diode placement

The purpose of diode monitoring of TSET is to verify delivery of the prescription dose and to assess the dose uniformity. A simple QA check of output constancy can be done before each treatment with a diode placed at a marked location on the TSET stand and irradiated by the calibration-size horizontal field. In vivo diode readings at the prescription point confirm the delivery of the prescription dose, while in vivo measurements at other locations assess uniformity. Dose to the top of the scalp, the perineum, and the axilla are usually lower than the prescription. In vivo diode readings at these sites help determine the need for and the size of a boost. Dose to the hands or feet is often too high because they are thin and receive dose from all six directions. For these sites,

diode readings help determine whether to add plastic compensators or bolus to reduce the dose.

Often, TSET treatments deliver the six dual fields in 2 days, alternating between two sets of three dual fields on different days.^{102,103} In this case, diode readings for the monitored sites should be taken on both days 1 and 2, and the sum of the readings for each site on the 2 days is compared with the prescription.

13 ESTABLISHING A DIODE-BASED IN VIVO DOSIMETRY PROGRAM

This section is directed to physicists who are new to in vivo dosimetry and/or to those who are beginning to supplement TLD with diodes. The ESTRO report²⁴ provides a valuable summary of the experiences of seven large European institutions. References particularly relevant to the United States or to small and mid-size clinics include 3, 6, 19, 20, 34, 44, 60, 65, 67, and 104.

13.1 Make pre-purchase decisions

Refer to section 3 of this report. Before purchasing the equipment, physicists and physicians should formulate the short- and long-term goals of the program including disease sites, measurement frequency, action levels, and resultant actions. Some commonly used schedules are:

1. Entrance measurements for each new or significantly changed photon field within the first 1 to 3 treatment sessions.
2. Same as 1, but include electron fields.
3. Entrance and exit measurements for a selected set of new photon fields within the first 1 to 3 treatment sessions.
4. One of the above with measurements repeated later in the course of treatment.
5. Entrance measurements at the prescription point level for all TBI treatments.
6. Dose-uniformity measurements (entrance and exit at ~5 different anatomical sites) for the first 1 or 2 TBI treatments and prescription point entrance measurements for all treatments.

Consider who will be involved in the program and what their involvement will be. Who will place the diodes, record the readings, obtain hardcopy, and review the readings? These considerations have an impact on the configuration of the system that is purchased.

13.2 Decide personnel responsibilities

Typical personnel responsibilities for a mid-size department are listed below.

Physicist(s): Overall responsibility for the program, including acceptance, commissioning, periodic QA, establishing action levels (in consultation with physician(s)), design of paper or electronic worksheets, in-servicing other personnel. Shares (with dosimetrists) responsibility for checking the calculations that will be compared with the diode measurements. Reviews or supervises review of the measurement results. Investigates measurements which fall outside the action levels, notifies the physician if treatment errors occurred or if the cause of the discrepancy is not understood and discusses remedial actions. TG-62 suggests that one physicist have primary responsibility for the diode program and that at least one qualified backup person be designated.

Dosimetrist(s): Calculates the quantities for comparison with diode readings and prepares the worksheet and assists physicists in investigating measurements outside of action levels. Shares other responsibilities as designated by the physicist(s).

Therapists(s): Places diodes, records the results, performs simple calculations to compare measured with expected results, and informs the physicist if a result exceeds tolerance.

Physician(s): Formally requests in vivo dosimetry and reviews each patient's in vivo dosimetry record after physics review is completed. Works with the physicist to establish the types of cases to measure, the measurement frequency, and the action levels. Determines the remedies when treatment errors are found.

13.3 Develop a reporting format

Decide how the measured and expected diode readings will be compared and design a paper or electronic worksheet to expedite quick comparison (see section 8). To help the therapist quickly recognize a problem, the worksheet should specify the range of acceptable readings for each field, based on your action levels. Formal documentation requires dated signatures of the staff who prepared and checked the worksheet, placed the diodes, and recorded the measurements.

13.4 Accept and commission the system

See sections 4 through 6 for details. When commissioning the system, it is advisable to spot-check the correction factors discussed in section 6, even if your clinical goal has a broad (e.g., 10%) action level. Commissioning is a good way to “kick the tires” of the new equipment and to familiarize yourself with its limitations.

13.5 Getting started: types of cases and in vivo measurement schedule

Expect a learning curve for everyone involved. Even if the ultimate goal of the in vivo dosimetry program is ambitious, it is best to start with simple treat-

ment techniques at sites without severe tissue or dosimetric inhomogeneities (e.g., whole brain, unwedged pelvic treatments), to compare measurements with hand calculations and with treatment planning system results, and to apply lenient initial action levels⁶ for the first few (e.g., 10) patients.

13.6 Simulate treatment geometries in phantom

Before “going clinical,” perform diode measurements on slab and/or anatomical phantoms for fields that simulate the treatments in terms of SSD, field size, accessories, and dose. Comparing these measurements with ion chamber measurements and with expected values based on manual and/or treatment planning system calculations gives information about the best performance you can expect.^{3,5,19,65,66,76,81} If TLD in vivo dosimetry is in use and is trusted, comparison of diode and TLD helps identify problems and to build confidence in the diode system.

13.7 Problem measurement sites

Anticipate problems at anatomical sites with steep slopes (head and neck, breast) and in wedged fields, where precise diode placement is critical to achieving agreement between measurement and calculation. These are not good sites with which to begin an in vivo dosimetry program. See section 9 and the references therein for discussion of placement issues. A diode placement practice session with involved therapists is helpful.

13.8 Electrons

Diode in vivo dosimetry has been found to be convenient and valuable for verifying, in real time, the dose delivery accuracy of electron beam treatments, which are often done as clinical setups. However, one should be aware of the dose perturbation (cf. section 9 and figure 9).

13.9 Action levels

If the goal of the in vivo dosimetry program is to detect large errors and prevent potential misadministrations, it is sufficient to set a single generous action level. As described in reference 19, an action level of $\pm 7\%$ can detect incorrect daily dose, wedge, beam energy, and confusion of SAD and SSD setups. If the program aims at tighter levels, many clinics find $\pm 5\%$ to be both practical and useful. There can be two action levels—a moderate (e.g., 5%) level for further investigation and a wider level (e.g., 10%) for immediate action or narrow action levels for simple treatments and wider ones for the problem measurement sites. Depending on the initial phantom measurements (the best you can

expect), on early clinical measurements and on long-term goals, you can later diversify the treatment techniques where you use diode dosimetry and/or tighten the action levels.

13.10 Establish reporting and follow-up procedures

These procedures include who should be called for problems and who reviews the vast majority of readings that are not problematic. It is important that the therapists have clear information as to who to contact in the event of a problem (e.g., name, pager, phone number).

Before clinical implementation, be prepared with a plan of actions to take if the action level is exceeded. For a review of strategies adopted by different groups in Europe, see reference 24 and elsewhere.^{20,44,63,65} A sample strategy adapted from reference 65 is described below.

1. Discrepancies exceeding 10% are immediately reviewed. The therapist contacts a designated member of the physics staff to review the setup, including diode placement, with the patient in treatment position. If no setup problem is observed, the physicist reviews the chart and MU calculations. If necessary, phantom measurements are performed using the same diodes, fields, SSD, and MU prior to the next treatment. In vivo diode measurements are repeated at the next treatment session with corrections to setup, diode placement, or MU as necessary and with a physicist present.
2. For discrepancies between 5% and 10%, a second therapist checks the setup, records the treatment parameters (SSD, field size, energy, treatment accessories), and takes the chart to the physicist for further investigation. In vivo measurements are repeated at the next treatment with the assistance of a physics staff member who is familiar with diode placement issues.
3. Treatment errors discovered through in vivo dosimetry are discussed with the physician and, in general, handled as are any other treatment errors at the clinic.
4. Measurements within tolerances are reviewed by a designated member of the physics staff before the patient has received more than five treatments or 20% of the prescribed treatment course. The worksheet or report that contains the comparison of calculated and measured doses is signed by the therapist, the reviewing physicist, and finally reviewed and signed by the physician.

13.11 In-service personnel

Train the therapists, with particular attention to the following points:

1. How to set up and take down the system.

2. Placement of the diodes: Diode orientation relative to patient skin, central axis vs. off-axis points.
3. Placement in wedged fields (both on and off-axis).
4. How to document the placement.
5. Use of the reporting form or spreadsheet.
6. Understanding the action levels.
7. What to do (and who to call) when the results are outside the range.
8. Care of the detectors, cables, and in-room electronics.

Expect to provide in-service training for new therapists and to provide “refresher courses” when new treatment sites, beam arrangements, or equipment are introduced for diode dosimetry. Reports^{6,20,34,62,66,70,81} agree that many out-of-tolerance measurements are related to diode placement. Therefore, it is important that personnel who place the diodes be thoroughly instructed as to proper diode positioning, especially in regions with large surface curvature, in wedged fields, and in fields where the central axis is under or close to a block edge. Written procedures are recommended.

Train the dosimetrists and involved physicists to prepare the diode in vivo dosimetry form and to calculate and check the expected diode readings or the reference point dose from the prescription dose and treatment plan.

13.12 Continuing QA

Continuing QA is discussed in section 7 of this report (section 11 for TBI). It is advised that a QA record or spreadsheet be maintained for improving the program, tracing problems, and clinical research.

13.13 Time estimates

It is generally agreed that diode in vivo dosimetry results in a small increase in treatment time (5 to 10 minutes, depending on complexity) at the measurement session.^{4,6,19} However, initiating and maintaining a diode in vivo dosimetry program is labor intensive and costly in terms of staff time. The physicists, physicians, and administrators of clinics intending to implement diode in vivo dosimetry should be realistic in facing the demands placed on personnel by such an effort.

The ESTRO report²⁴ quotes acceptance/commissioning times ranging from 4 to 10 hours per diode. A survey of members of TG-62 gave acceptance/commissioning times ranging from approximately 4 to 14 hours/diode. Time to develop forms and procedures and staff training are not included in these estimates although such time is clearly needed. Estimates of weekly physics staff work by members of TG-62 run between 1 and 10 hours while ongoing QA can easily contribute an additional 20 hours/year. One task group member, who managed a comprehensive diode in vivo dosimetry program, estimated that the

program utilized approximately 0.4 full-time equivalents (FTE)/year once it was underway and required 0.55 FTE for startup effort. This program involved a total of four linacs (three at one facility, one at another) treating a total of 140 to 150 patients daily with in vivo dosimetry being done on all new fields and, thereafter, weekly. A similar estimate (0.4 FTE) is reported by the Netherlands Cancer Institute for a program with tight tolerance levels in three-dimensional conformal radiation therapy (3DCRT) patients.⁴

14 REFERENCES

1. M. Essers and B. J. Mijnheer. "In vivo dosimetry during external photon beam radiotherapy." *Int J Radiat Oncol Biol Phys* 43:245–249 (1999).
2. M. Essers. "In vivo dosimetry in radiotherapy. Development, use and evaluation of accurate patient dose verification methods." Thesis, Free University, Amsterdam (1996).
3. D. P. Fontenla, R. Yaparalvi, C.-S. Chui, E. Briot. "The use of diode dosimetry in quality improvement of patient care in radiation therapy." *Med Dosim* 21:235–241 (1996).
4. J. H. Lanson, M. Essers, G. J. Meijer, A. W. H. Minken, G. J. Uiterwaal, B. J. Mijnheer. "In vivo dosimetry during conformal radiotherapy: Requirements for and findings of a routine procedure." *Radiother Oncol* 52:51–59 (1999).
5. G. Leunens, J. Van Dam, A. Dutreix, E. Van Der Schueren. "Quality assurance in radiotherapy by in vivo dosimetry. I. Entrance dose measurements, a reliable procedure." *Radiother Oncol* 17:141–151 (1990).
6. M. Voordeckers, H. Goossens, J. Rutten, W. Van den Bogaert. "The implementation of in vivo dosimetry in a small radiotherapy department." *Radiother Oncol* 47:45–48 (1998).
7. G. Leunens, J. Verstraete, A. Dutreix, E. van der Schueren. "Assessment of dose inhomogeneity at target level by in vivo dosimetry: Can the recommended 5% accuracy in the dose delivered to the target volume be fulfilled in daily practice?" *Radiother Oncol* 25:242–250 (1992).
8. A. Feldman and F. M. Edwards. "The routine use of personal patient dosimeters is of little value in detecting therapeutic misadministrations; Point/Counterpoint." *Med Phys* 28:295–297 (2001).
9. www.fda.gov/cdrh/ocd/panamaradexp.html.
10. S. Vatnitsky, P. O. Lopez, J. Izewska, A. Meghzifene, V. Levin. "The radiation overexposure of radiotherapy patients in Panama 15 June 2001." *Radiother Oncol* 60:237–238 (2001).
11. "Investigation of an accidental exposure of radiotherapy patients in Panama, Report of a Team of Experts." 26 May–1 June 2001. IAEA Report (2001).
12. G. J. Kutcher, L. Coia, M. Gillin, W. F. Hanson, S. Leibel, R. J. Morton, J. R. Palta, J. A. Purdy, L. E. Reinstein, G. K. Svensson, M. Weller, L. Wingfield. "Comprehensive QA for radiation oncology: Report of AAPM Radiation Therapy Committee Task Group 40." *Med Phys* 21:581–618 (1994). Also available as AAPM Report No. 46.

13. W. P. N. Mayles, S. Heisig, and H. M. O. Mayles. "Treatment Verification and in vivo Dosimetry" in *Radiotherapy Physics* by J. R. Williams and D. I. Thwaites. Oxford: Oxford University Press, pp. 227–251, 1993.
14. J. Van Dam and G. Marinello. Methods for in vivo Dosimetry in External Radiotherapy. ESTRO Booklet on Physics for Clinical Radiotherapy No. 1. Garant (Leuven-Apeldoorn) (1994). (Check for PDF version at www.estroweb.org).
15. G. Rikner and E. Grusell. "Effect of radiation damage on p-type silicon detectors." *Phys Med Biol* 28:1261–1267 (1983).
16. G. Rikner and E. Grusell. "General specification for silicon semi-conductors for use in radiation dosimetry." *Phys Med Biol* 32:1109–1117 (1987).
17. G. Rikner. "Silicon diode as detectors in relative dosimetry of photon, electron and proton radiation fields." Ph.D. Thesis, University of Uppsala, Sweden (1983).
18. Th. Loncol, J. L. Greffe, S. Vynckier, P. Scalliet. "Entrance and exit dose measurements with semiconductors and thermoluminescent dosimeters: A comparison of methods and in vivo results." *Radiother Oncol* 41:179–187 (1996).
19. P. C. Lee, J. M. Sawicka, and G. P. Glasgow. "Patient dosimetry quality assurance program with a commercial diode system." *Int J Radiat Oncol Biol Phys* 29:1175–1182 (1994).
20. S. Howlett, L. Duggan, S. Bazley, T. Kron. "Selective in vivo dosimetry in radiotherapy using p-type semiconductor diodes: A reliable quality assurance procedure." *Med Dosim* 24:53–56 (1999).
21. G. J. Meijer, A. W. H. Minken, K. M. van Ingen, B. Smulders, H. Uiterwaal, B. J. Mijneer. "Accurate in vivo dosimetry of a randomized trial of prostate cancer irradiation." *Int J Radiat Oncol Biol Phys* 49:1409–1418 (2001).
22. J. R. Greig, R. W. Miller, P. Okunieff. "An approach to dose measurement for total body irradiation." *Int J Radiat Oncol Biol Phys* 36:463–468 (1996).
23. B. Planskoy, P. D. Tapper, A. M. Bedford, F. M. Davis. "Physical aspects of total-body irradiation at the Middlesex Hospital (UCL group of hospitals), London 1988–1993, II. In vivo planning and dosimetry." *Phys Med Biol* 41:2327–2343 (1996).
24. D. Huyskens, R. Bogaerts, J. Verstraete, M. Lööf, H. Nyström, C. Fiorino, S. Broggi, N. Jornet, M. Ribas, D. I. Thwaites. Practical Guidelines for the Implementation of in vivo Dosimetry with Diodes in External radiotherapy with Photon Beams (Entrance Dose). ESTRO Physics for Clinical Radiotherapy Booklet No. 5 (2001). (Check for PDF version at www.estro.be).
25. R. P. Parker. "Semiconductor nuclear radiation detectors." *Phys Med Biol* 15:605–620 (1970).
26. T. Guldbrandsen and C. B. Madsen. "Radiation dosimetry by means of semiconductors." *Acta Radiol* 58:226 (1961).
27. K. Sharf and K. Tarczy. "Steady-state response of silicon radiation detectors of diffused p-n junction-type to x-rays. 1R: Photo-voltage mode of operation." *J Res National Bureau of Standards* 68A:683 (1964).
28. S. C. Klevenhagen. "Temperature response of silicon surface barrier semiconductor detector operated in the dc-short circuit configuration." *Acta Radiol* 12:124–144 (1973).
29. Edward S. Yang. *Microelectronic Devices*. Chapters 2 and 3, New York: McGraw-Hill, Inc. 1988.

30. Robert F. Pierret. *Advanced Semiconductor Fundamentals*. 2nd Ed., New York: Prentice Hall, 2002.
31. J. Shi, W. E. Simon, T. C. Zhu. "Modeling the instantaneous dose rate dependence of radiation diode detectors." *Med Phys* 30:2509–2519 (2003).
32. E. Grusell and G. Rikner. "Evaluation of temperature effects in p-type silicon detectors." *Phys Med Biol* 31:527–534 (1986).
33. J. Shi. "Characteristics of the Si diode as a radiation detector for the application of in vivo dosimetry." Thesis, Florida Institute of Technology (May 1995).
34. R. Alecu, M. Alecu, T. G. Ochrán. "A method to improve the effectiveness of diode in vivo dosimetry." *Med Phys* 25:746–749 (1998).
35. J. Shi, W. E. Simon, T. C. Zhu, and S. Johnsen. "Investigation of scatter contribution to the diode detector SSD dependence by changing accelerator gun current." *Med Phys* 24:1066 (1997).
36. J. Shi, W. E. Simon, L. Ding, D. Saini, S. Rose. "Effects of buildup thickness and material to diode detector SSD dependence." *Med Phys* 26:1127 (1999).
37. N. Jornet, M. Ribas, T. Eudaldo. "In vivo dosimetry: Intercomparison between p-type based and n-type based diodes for the 16-25 MV energy range." *Med Phys* 27:1287–1293 (2000).
38. R. L. Dixon and K. E. Ekstrand. "Gold and Platinum Doped Radiation Resistant Silicon Diode Detectors." Proceedings of the VIII International Conference on Solid State Dosimetry, Oxford, UK, August 1986, pp. 527–530.
39. R. O. Carlson, Y. S. Sun, and H. Assalit. "Lifetime control in silicon power devices by electron or gamma irradiation." *IEEE Transactions on Electron Devices*, Vol. ED-24, No. 8, p. 1104, August 1977.
40. J. Shi, W. E. Simon, S. Johnsen. "A study of n and p type diode detectors after very high radiation dose from electron and photon beams." *Med Phys* 25:A192 (1998).
41. E. Grusell and G. Rikner. "Linearity with dose-rate of low resistivity p-type silicon semiconductor detectors." *Phys Med Biol* 38:785–792 (1993).
42. J. Van Dam, G. Leunens, and A. Dutreix. "Correlation between temperature and dose rate dependence of semiconductor response: influence of accumulated dose." *Radiother Oncol* 19:345–351 (1990).
43. A. S. Saini and T. C. Zhu. "Temperature dependence of commercially available diode detectors." *Med Phys* 29:622–630 (2002).
44. P. A. Jursinic. "Implementation of an in vivo diode dosimetry program and changes in diode characteristics over a four-year clinical history." *Med Phys* 28:1718–1726 (2001).
45. K. T. Welsh and L.E. Reinstein. "The thermal characteristics of different diodes on in vivo patient dosimetry." *Med Phys* 28:844–849 (2001).
46. J. Shi, W. E. Simon, L. Ding, and D. Saini. "Important Issues Regarding Diode Performance In Radiation Therapy Applications." Digest of Papers of the 2000 World Congress on Medical Physics and Biomedical Engineering and the Proceedings of the 22nd Annual International Conference of the IEEE Engineering in Medicine and Biology Society, 0-7803-6468-6 © 2000 IEEE, Chicago (2000).
47. E. Grusell and G. Rikner. "Radiation damage induced dose-rate non linearity in an n-type silicon detector." *Acta Radiol Oncol* 23:465–469 (1984).

48. J. N. Eveling, A. M. Morgan, and W. G. Pitchford. "Commissioning a p-type silicon diode for use in clinical electron beams." *Med Phys* 26:100–107 (1999).
49. D. Marre and G. Marinello. "Comparison of p-type commercial electron diodes for in vivo dosimetry." *Med Phys* 31:50–56 (2004).
50. C. B. Saw, J. Shi, D. H. Hussey. "Energy dependence of a new solid state diode for low energy photon beam dosimetry." *Med Dosim* 23:95–97 (1998).
51. D. Georg, B. De Ost, M. T. Hoornaert, P. Pilette, J. Van Dam, M. Van Dycke, D. Huyskens. "Build-up modification of commercial diodes for entrance dose measurements in 'higher energy' photon beams." *Radiother Oncol* 51:249–256 (1999).
52. A. Saini and T. C. Zhu. "Dosimetric characteristics of p-type QED diode detectors used for in vivo dosimetry." *Med Phys* 25:A177 (1998).
53. F. Khan. *The Physics of Radiation Therapy*, 2nd Edition. Ch 10. Baltimore: Williams & Wilkins, 1994.
54. J. Shi, W. E. Simon, L. Ding. "Influence of buildup thickness to the field size dependence of diode detector and correlation with the SSD dependence." *Med Phys* 28 (6):1221 (2001).
55. A. Sen, E. I. Parsai, S. W. McNeeley, K. M. Ayyangar. "Quantitative assessment of beam perturbations caused by silicon diodes used for in vivo dosimetry." *Int J Radiat Oncol Biol Phys* 36:205–211 (1996).
56. D. M. D. Frye and S. N. Rustgi. "Diode verification of routine electron-beam treatments." *Med Dosim* 24:43–48 (1999).
57. R. W. Luse, J. Eenmaa, T. Kwiatkowski, D. Schumacher. "In vivo diode dosimetry for total marrow irradiation." *Int J Radiat Oncol Biol Phys* 36:189–195 (1996).
58. J. G. Wierzbicki and D. S. Waid. "Large discrepancies between calculated Dmax and diode readings for small field sizes and small SSDs of 15 MV photon beams." *Med Phys* 25:245–246 (1998).
59. R. Alecu, J. Feldmeier, M. Alecu. "Dose perturbations due to in vivo dosimetry with diodes." *Radiother Oncol* 42:289–291 (1997).
60. C. Li, L. S. Lamel and D. Tom. "A patient dose verification program using diode detectors." *Med Dosim* 20:209–214 (1995).
61. V. C. Colussi, A. S. Beddar, T. J. Kinsella, C. H. Sibata. "In vivo dosimetry using a single diode for megavoltage photon beam radiotherapy: Implementation and response characterization." *J Appl Clin Med Phys* 2:210–218 (2001).
62. C. J. Millwater, A. S. MacLeod, D. I. Thwaites. "In vivo semiconductor dosimetry as part of routine quality assurance." *Br J Radiol* 71:661–668 (1998).
63. D. P. Fontenla, J. Curran, R. Yaparalvi, B. Vikram. "Customization of a radiation management system to support in vivo patient dosimetry using diodes." *Med Phys* 23:1425–1429 (1996).
64. P. R. Almond, P. J. Biggs, B. M. Coursey, W. F. Hanson, M. S. Huq, R. Nath, D. W. O. Rogers. "AAPM's TG-51 protocol for clinical reference dosimetry of high-energy photon and electron beams." *Med Phys* 26:1847–1870 (1999). Also available as AAPM Report No. 67.
65. R. Alecu, T. Loomis, J. Alecu, T. Ochran. "Guidelines on the implementation of diode in vivo dosimetry programs for photon and electron external beam therapy." *Med Dosim* 24:5–12 (1999).

66. R. Yaparpalvi, D. P. Fontenla, B. Vikram. "Clinical experience with routine diode dosimetry for electron beam radiotherapy." *Int J Radiat Oncol Biol Phys* 48:1259–1265 (2000).
67. R. Yaparpalvi, D. P. Fontenla, L. Yu, P. P. Lai, B. Vikram. "Radiation therapy of breast carcinoma: Confirmation of prescription dose using diodes." *Int J Radiat Oncol Biol Phys* 35:173–183 (1996).
68. M. Essers, J. H. Lanson, and B. J. Mijnheer. "In vivo dosimetry during conformal therapy of prostatic cancer." *Radiother Oncol* 29:271–279 (1993).
69. A. Rizzotti, C. Compri, G. F. Garusi. "Dose evaluation to patients irradiated by ^{60}Co beams by means of direct measurement on the incident and on the exit surfaces." *Radiother Oncol* 3:279–283 (1985).
70. A. Adeyemi and J. Lord. "An audit of radiotherapy patient doses measured with in vivo semiconductor detectors." *Br J Radiol* 70:399–408 (1997).
71. J. N. Verney and A. M. Morgan. "Evaluation of in vivo dose measurements for patients undergoing electron boost treatments." *Radiother Oncol* 59:293–296 (2001).
72. N. Jornet, M. Ribas, T. Eudaldo. "Calibration of semiconductor detectors for dose assessment in total body irradiation." *Radiother Oncol* 38:247–251 (1996).
73. S. Heukelom, J. H. Lanson and B. J. Mijnheer. "Comparison of entrance and exit dose measurements using ionization chambers and silicon diodes." *Phys Med Biol* 36:47–59 (1991).
74. H. E. Johns and J. R. Cunningham. *The Physics of Radiology*, 4th ed. Springfield, IL: Charles C Thomas, pp. 275–277, 1983.
75. J. A. Purdy. "Buildup/surface dose and exit dose measurements for a 6 MV linear accelerator." *Med Phys* 13:259–262 (1986).
76. L. Cozzi and A. Fogliata-Cozzi. "Quality assurance in radiation oncology. A study of feasibility and impact on action levels of an in vivo dosimetry program during breast cancer irradiation." *Radiother Oncol* 47:29–36 (1998).
77. R. J. Meiler and M. B. Podgorsak. "Characterization of the response of commercial diode detectors used for in vivo dosimetry." *Med Dosim* 22:31–37 (1997).
78. X. R. Zhu. "Entrance dose measurements for in-vivo diode dosimetry: Comparison of correction factors for two types of commercial silicon diode detectors." *J Appl Clin Med Phys* 1:100–107 (2000).
79. G. Leunens, J. Van Dam, A. Dutreix and E. van der Scheuren. "Quality assurance in radiotherapy by in vivo dosimetry. 2. Determination of the target absorbed dose." *Radiother Oncol* 19:73–97 (1990).
80. P. A. Jursinic. "Changes in incident photon fluence of 6 and 18 MV x rays caused by blocks and block trays." *Med Phys* 26:2092–2098 (1999).
81. M. Essers, R. Keus, J. H. Lanson, B. J. Mijnheer. "Dosimetric control of conformal treatment of parotid gland tumors." *Radiother Oncol* 32:154–162 (1994).
82. F. Khan. "Total Skin Electron Therapy: Technique and Dosimetry" in *Advances in Radiation Oncology Physics*, AAPM Monograph No. 19, J.A. Purdy (ed.). New York: American Institute of Physics, pp. 466–479, 1992.
83. S. Heukelom, J. H. Lanson, B. J. Mijnheer, "In vivo dosimetry during pelvic treatment." *Radiother Oncol* 25:111–120, (1992).
84. R. L. Dixon and K. E. Ekstrand. "Gold and platinum doped radiation resistant silicon diode detectors." *Radiat Prot Dosim* 17:527–530 (1986).

85. G. Rikner. "Characteristics of a p-Si detector in high energy electron fields." *Acta Radiol Oncol* 3:279–283 (1985).
86. International Commission on Radiation Units and Measurements (ICRU). Report 50. "Prescribing, Recording and Reporting Photon Beam Therapy." Bethesda, MD: ICRU, 1993.
87. R. Boellaard, M. Essers, M. van Herk, B. J. Mijnheer. "New method to obtain the midplane dose using portal in vivo dosimetry." *Int J Radiat Oncol Biol Phys* 41:465–474 (1998).
88. D. Huyskens, J. Van Dam, A. Dutreix. "Midplane dose determination using in vivo dose measurements in combination with portal imaging." *Phys Med Biol* 39:1089–1101 (1994).
89. P. Mangili, C. Fiorino, A. Rosso, G. M. Cattaneo, R. Parisi, E. Villa, R. Calandrino, "In-vivo dosimetry by diode semiconductors in combination with portal films during TBI: Reporting a 5-year clinical experience." *Radiother Oncol* 52:269–276 (1999).
90. J. R. Marbach, M. R. Sontag, J. Van Dyk, A. B. Wolbarst. "Management of radiation oncology patients with implanted cardiac pacemakers: Report of AAPM Task Group No. 34." *Med Phys* 21:85–90 (1994). Also available as AAPM Report No. 45.
91. M. Stovall, C. R. Blackwell, J. Cundiff, D. H. Novack, J. R. Palta, L. K. Wagner, E. W. Webster, R. J. Shalek. "Fetal dose from radiotherapy with photon beams: Report of AAPM Radiation Therapy Committee Task Group No. 36." *Med Phys* 22:63–82 (1995).
92. S. Marcie, A. Costa, J. L. Lagrange. "Protection of testes during radiation treatment by irregular and focused fields of 25 MV x-rays: in vivo evaluation of the absorbed dose." *Med Dosim* 20:269–273 (1995).
93. T. C. Zhu, L. Ding, C. R. Liu, J. R. Palta, W. E. Simon, J. Shi. "Performance evaluation of a diode array for enhanced dynamic wedge dosimetry." *Med Phys* 24:1173–1180 (1997).
94. C. C. Ling, C. Burman, C. S. Chui, G. J. Kutcher, S. A. Leibel, T. LoSasso, R. Mohan, T. Bortfeld, L. Reinstein, S. Spirou, X. H. Wang, Q. Wu, M. Zelefsky and Z. Fuks. "Conformal radiation treatment of prostate cancer using inversely planned intensity modulated photon beams produced with dynamic multileaf collimation." *Int J Radiat Oncol Biol Phys* 35:721–730 (1996).
95. A. Van Esch, J. Bohsung, P. Sorvari, M. Tenhunen, M. Pausco, M. Iori, P. Engstrom, H. Nystrom, D. P. Huyksens. "Acceptance tests and quality control (QC) procedures for the clinical implementation of intensity modulated radiotherapy (IMRT) using inverse planning and the sliding window technique: experience from five radiotherapy departments." *Radiother Oncol* 65:53–70 (2002).
96. P. D. Higgins, P. Alaei, B. J. Gerbi, K. E. Dusenbery. "In vivo diode dosimetry for routine quality assurance in IMRT." *Med Phys* 30:3118–3123 (2003).
97. T. J. LoSasso. "Quality Assurance of IMRT" in *A Practical Guide to Intensity Modulated Radiation Therapy*. Madison, WI: Medical Physics Publishing, pp. 147–167, 2003.
98. P. A. Jursinic and B. E. Nelms. "A 2-D diode array and analysis software for verification of intensity modulated radiation therapy delivery." *Med Phys* 30:870–879 (2003).

99. J. Van Dyk, J. M. Galvin, G. P. Glasgow, E. B. Podgorsak. "The Physical Aspects of Total and a Half Body Photon Irradiation." AAPM Report No 17. New York: American Institute of Physics (1986).
100. B. Planskoy, A. M. Bedford, F. M. Davis, P. D. Tapper, L. T. Loverock, "Physical aspects of total-body irradiation at the Middlesex Hospital (UCL group of hospitals), London 1988–1993, I. Phantom measurements and planning methods." *Phys Med Biol* 41:2307–2326 (1996).
101. M. Ribas, N. Jornet, T. Eudaldo, D. Carabante, M. A. Duch, M. Ginjaume, G. Gomez de Segura, F. Sanchez-Doblado. "Midplane dose determination during total body irradiation using in vivo dosimetry." *Radiother Oncol* 49:91–98 (1998).
102. C. J. Karzmark, J. Anderson, P. Fessenden, G. Svensson, A. Buffa, F. Khan, K. Wright. "Total Skin Electron Therapy: Technique and Dosimetry." AAPM Report 23. New York: American Institute of Physics (1988).
103. R. S. Cox, R. J. Heck, P. Fessenden, C. J. Karzmark, and D. C. Rust. "Development of total-skin electron therapy at two energies." *Int J Radiat Oncol Biol Phys* 18:659–669 (1990).
104. M. B. Podgorsak, J. P. Balog, C. H. Sibata, A. K. Ho. "In vivo dosimetry using a diode detector system: Regarding Lee et al." *Int J Radiat Oncol Biol Phys* 32:556–557 (1995) and response by P. C. Lee, G. P. Glasgow. "In response to Dr. Podgorsak et al." *Int J Radiat Oncol Biol Phys* 32:557 (1995).
105. Intensity Modulated Radiation Therapy Collaborative Working Group. "Intensity-modulated radiotherapy: Current status and issues of interest." *Int J Radiat Oncol Biol Phys* 51:880–914 (2001).
106. A. S. Saini, T. C. Zhu, I. Rebo. "Dosimetric evaluation of new n-type Pt-doped QED diode detectors." *Med Phys* 30:1479 (2003).
107. E. E. Klein, D. A. Low, A. S. Meigooni, J. A. Purdy. "Dosimetry and clinical implementation of dynamic wedge." *Int J Radiat Oncol Biol Phys* 31:583–592 (1995).
108. G. Marinello. "Radiothermoluminescent Dosimeters and Diodes" in *Handbook of Radiotherapy Physics*, P. Mayles, J.C. Rosenwald, A. Nahum, Bristol: Institute of Physics Publishing, In press, 2004.
109. A. S. Saini and T. C. Zhu. "Dose rate and SDD dependence of commercially available diode detectors." *Med Phys* 31:914–924 (2004).

AAPM REPORT SERIES

- No. 1 "Phantoms for Performance Evaluation and Quality Assurance of CT Scanners" (1977)
- No. 3 "Optical Radiations in Medicine: A Survey of Uses, Measurement and Sources" (1977)
- No. 4 "Basic Quality Control in Diagnostic Radiology," AAPM Task Force on Quality Assurance Protocol (1977)
- No. 5 "AAPM Survey of Medical Physics Training Programs," Committee on the Training of Medical Physicists (1980)
- No. 6 "Scintillation Camera Acceptance Testing & Performance Evaluation," AAPM Nuclear Medicine Committee (1980)
- No. 7 "Protocol for Neutron Beam Dosimetry," AAPM Task Group #18 (1980)
- No. 8 "Pulse Echo Ultrasound Imaging Systems: Performance Tests & Criteria," P. Carson & J. Zagzebski (1980)
- No. 9 "Computer-Aided Scintillation Camera Acceptance Testing," AAPM Task Group of the Nuclear Medicine Committee (1982)
- No. 10 "A Standard Format for Digital Image Exchange," Baxter et al. (1982)
- No. 11 "A Guide to the Teaching of Clinical Radiological Physics to Residents in Radiology," AAPM Committee on the Training of Radiologists (1982)
- No. 12 "Evaluation of Radiation Exposure Levels in Cine Cardiac Catheterization Laboratories," AAPM Cine Task Force of the Diagnostic Radiology Committee (1984)
- No. 13 "Physical Aspects of Quality Assurance in Radiation Therapy," AAPM Radiation Therapy Committee Task Group #24, with contribution by Task Group #22 (1984)
- No. 14 "Performance Specifications and Acceptance Testing for X-Ray Generators and Automatic Exposure Control Devices" (1985)
- No. 15 "Performance Evaluation and Quality Assurance in Digital Subtraction Angiography," AAPM Digital Radiology/ Fluorography Task Group (1985)
- No. 16 "Protocol for Heavy Charged-Particle Therapy Beam Dosimetry," AAPM Task Group #20 of the Radiation Therapy Committee (1986)
- No. 17 "The Physical Aspects of Total and Half Body Photon Irradiation," AAPM Task Group #29 of the Radiation Therapy Committee (1986)
- No. 18 "A Primer on Low-Level Ionizing Radiation and its Biological Effects," AAPM Biological Effects Committee (1986)
- No. 19 "Neutron Measurements Around High Energy X-Ray Radiotherapy Machines," AAPM Radiation Therapy Task Group #27 (1987)
- No. 20 "Site Planning for Magnetic Resonance Imaging Systems," AAPM NMR Task Group #2 (1987)
- No. 21 "Specification of Brachytherapy Source Strength," AAPM Radiation Therapy Task Group #32 (1987)
- No. 22 "Rotation Scintillation Camera Spect Acceptance Testing and Quality Control," Task Group of Nuclear Medicine Committee (1987)
- No. 23 "Total Skin Electron Therapy: Technique and Dosimetry," AAPM Radiation Therapy Task Group #30 (1988)
- No. 24 "Radiotherapy Portal Imaging Quality," AAPM Radiation Therapy Task Group #28 (1988)

- No. 25 “Protocols for the Radiation Safety Surveys of Diagnostic Radiological Equipment,” AAPM Diagnostic X-Ray Imaging Committee Task Group #1 (1988)
- No. 26 “Performance Evaluation of Hyperthermia Equipment,” AAPM Hyperthermia Task Group #1 (1989)
- No. 27 “Hyperthermia Treatment Planning,” AAPM Hyperthermia Committee Task Group #2 (1989)
- No. 28 “Quality Assurance Methods and Phantoms for Magnetic Resonance Imaging,” AAPM Nuclear Magnetic Resonance Committee Task Group #1, Reprinted from *Medical Physics*, Vol. 17, Issue 2 (1990)
- No. 29 “Equipment Requirements and Quality Control for Mammography,” AAPM Diagnostic X-Ray Imaging Committee Task Group #7 (1990)
- No. 30 “E-Mail and Academic Computer Networks,” AAPM Computer Committee Task Group #1 (1990)
- No. 31 “Standardized Methods for Measuring Diagnostic X-Ray Exposures,” AAPM Diagnostic X-Ray Imaging Committee Task Group #8 (1991)
- No. 32 “Clinical Electron-Beam Dosimetry,” AAPM Radiation Therapy Committee Task Group #25, Reprinted from *Medical Physics*, Vol. 18, Issue 1 (1991)
- No. 33 “Staffing Levels and Responsibilities in Diagnostic Radiology,” AAPM Diagnostic X-Ray Imaging Committee Task Group #5 (1991)
- No. 34 “Acceptance Testing of Magnetic Resonance Imaging Systems,” AAPM Nuclear Magnetic Resonance Task Group #6, Reprinted from *Medical Physics*, Vol. 19, Issue 1 (1992)
- No. 35 “Recommendations on Performance Characteristics of Diagnostic Exposure Meters,” AAPM Diagnostic X-Ray Imaging Task Group #6, Reprinted from *Medical Physics*, Vol. 19, Issue 1 (1992)
- No. 36 “Essentials and Guidelines for Hospital Based Medical Physics Residency Training Programs,” AAPM Presidential AD Hoc Committee (1992)
- No. 37 “Auger Electron Dosimetry,” AAPM Nuclear Medicine Committee Task Group #6, Reprinted from *Medical Physics*, Vol. 19, Issue 1 (1993)
- No. 38 “The Role of the Physicist in Radiation Oncology,” Professional Information and Clinical Relations Committee Task Group #1 (1993)
- No. 39 “Specification and Acceptance Testing of Computed Tomography Scanners,” Diagnostic X-Ray Imaging Committee Task Group #2 (1993)
- No. 40 “Radiolabeled Antibody Tumor Dosimetry,” AAPM Nuclear Medicine Committee Task Group #2, Reprinted from *Medical Physics*, Vol. 20, Issue 2, Part 2 (1993)
- No. 41 “Remote Afterloading Technology,” Remote Afterloading Technology Task Group #41 (1993)
- No. 42 “The Role of the Clinical Medical Physicist in Diagnostic Radiology,” Professional Information and Clinical Relations Committee Task Group #2 (1994)
- No. 43 “Quality Assessment and Improvement of Dose Response Models,” (1993).
- No. 44 “Academic Program for Master of Science Degree in Medical Physics,” AAPM Education and Training of Medical Physicists Committee (1993)
- No. 45 “Management of Radiation Oncology Patients with Implanted Cardiac Pacemakers,” AAPM Task Group #4, Reprinted from *Medical Physics*, Vol. 21, Issue 1 (1994)

- No. 46 “Comprehensive QA for Radiation Oncology,” AAPM Radiation Therapy Committee Task Group #40, Reprinted from *Medical Physics*, Vol. 21, Issue 6 (1994)
- No. 47 “AAPM Code of Practice for Radiotherapy Accelerators,” AAPM Radiation Therapy Task Group #45, Reprinted from *Medical Physics*, Vol. 21, Issue 7 (1994)
- No. 48 “The Calibration and Use of Plane-Parallel Ionization Chambers for Dosimetry of Electron Beams,” AAPM Radiation Therapy Committee Task Group #39, Reprinted from *Medical Physics*, Vol. 21, Issue 8 (1994)
- No. 49 “Dosimetry of Auger-Electron-Emitting Radionuclides,” AAPM Nuclear Medicine Task Group #6, Reprinted from *Medical Physics*, Vol. 21, Issue 12 (1994)
- No. 50 “Fetal Dose from Radiotherapy with Photon Beams,” AAPM Radiation Therapy Committee Task Group #36, Reprinted from *Medical Physics*, Vol. 22, Issue 1 (1995)
- No. 51 “Dosimetry of Interstitial Brachytherapy Sources,” AAPM Radiation Therapy Committee Task Group #43, Reprinted from *Medical Physics*, Vol. 22, Issue 2 (1995)
- No. 52 “Quantitation of SPECT Performance,” AAPM Nuclear Medicine Committee Task Group #4, Reprinted from *Medical Physics*, Vol. 22, Issue 4 (1995)
- No. 53 “Radiation Information for Hospital Personnel,” AAPM Radiation Safety Committee (1995)
- No. 54 “Stereotactic Radiosurgery,” AAPM Radiation Therapy Committee Task Group #42 (1995)
- No. 55 “Radiation Treatment Planning Dosimetry Verification,” AAPM Radiation Therapy Committee Task Group #23 (1995), \$48, (Includes 2 disks, ASCII format).
- No. 56 “Medical Accelerator Safety Considerations,” AAPM Radiation Therapy Committee Task Group #35, Reprinted from *Medical Physics*, Vol. 20, Issue 4 (1993)
- No. 57 “Recommended Nomenclature for Physical Quantities in Medical Applications of Light,” AAPM General Medical Physics Committee Task Group #2 (1996)
- No. 58 “Managing the Use of Fluoroscopy in Medical Institutions,” AAPM Radiation Protection Committee Task Group #6 (1998)
- No. 59 “Code of Practice for Brachytherapy Physics,” AAPM Radiation Therapy Committee Task Group #56, Reprinted from *Medical Physics*, Vol. 24, Issue 10 (1997)
- No. 60 “Instrumentation Requirements of Diagnostic Radiological Physicists,” AAPM Diagnostic X-Ray Committee Task Group #4 (1998)
- No. 61 “High Dose Brachytherapy Treatment Delivery,” AAPM Radiation Therapy Committee Task Group #59, Reprinted from *Medical Physics*, Vol. 25, Issue 4 (1998)
- No. 62 “Quality Assurance for Clinical Radiotherapy Treatment Planning,” AAPM Radiation Therapy Committee Task Group #53, Reprinted from *Medical Physics*, Vol. 25, Issue 10 (1998)
- No. 63 “Radiochromic Film Dosimetry,” AAPM Radiation Therapy Committee Task Group #55, Reprinted from *Medical Physics*, Vol. 25, Issue 11 (1998)

- No. 64 "A Guide to the Teaching Of Clinical Radiological Physics To Residents in Diagnostic and Therapeutic Radiology," Revision of AAPM Report #11, AAPM Committee on the Training of Radiologists (January 1999)
- No. 65 "Real-Time B-Mode Ultrasound Quality Control Test Procedures," AAPM Ultrasound Task Group #1, Reprinted from *Medical Physics*, Vol. 25, Issue 8 (1998)
- No. 66 "Intravascular Brachytherapy Physics," AAPM Radiation Therapy Committee Task Group #60, Reprinted from *Medical Physics*, Vol. 26, Issue 2 (1999)
- No. 67 "Protocol for Clinical Reference Dosimetry of High-Energy Photon and Electron Beams," AAPM Task Group #51, Reprinted from *Medical Physics*, Vol. 26, Issue 9 (1999)
- No. 68 "Permanent Prostate Seed Implant Brachytherapy," AAPM Medicine Task Group #64, Reprinted from *Medical Physics*, Vol. 26, Issue 10 (1999)
- No. 69 "Recommendations of the AAPM on 103Pd Interstitial Source Calibration and Dosimetry: Implications for Dose Specification and Prescription," Report of the Low Energy Interstitial Brachytherapy Dosimetry Subcommittee of the Radiation Therapy Committee, Reprinted from *Medical Physics*, Vol. 27, Issue 4 (2000)
- No. 70 "Cardiac Catherization Equipment Performance," AAPM Task Group #17 Diagnostic X-ray Imaging Committee (February 2001)
- No. 71 "A Primer for Radioimmunotherapy and Radionuclide Therapy," AAPM Task Group #7 Nuclear Medicine Committee (April 2001)
- No. 72 "Basic Applications of Multileaf Collimators," AAPM Task Group #50 Radiation Therapy Committee (July 2001)
- No. 73 "Medical Lasers: Quality Control, Safety, Standards, and Regulations," Joint Report of Task Group #6 AAPM General Medical Physics Committee and ACMP (July 2001)
- No. 74 "Quality Control in Diagnostic Radiology," Report of AAPM Task Group 12, Diagnostic X-ray Imaging Committee (2002)
- No. 75 "Clinical Use of Electronic Portal Imaging," AAPM Radiation Therapy Committee Task Group #58. Reprinted from *Medical Physics*, Vol. 28, Issue 5 (2001)
- No. 76 "AAPM Protocol for 40-300 kV X-ray Beam Dosimetry in Radiotherapy and Radiobiology," AAPM Radiation Therapy Committee Task Group #61. Reprinted from *Medical Physics*, Vol. 28, Issue 6 (2001)
- No. 77 "Practical Aspects of Functional MRI," AAPM NMR Task Group #8. Reprinted from *Medical Physics*, Vol. 29, Issue 8 (2002)
- No. 78 "Proton Magnetic Resonance Spectroscopy in the Brain: Report of AAPM Magnetic Resonance Task Group #9." Reprinted from *Medical Physics*, Vol. 29, Issue 9 (2002)
- No. 79 "Academic Program Recommendations For Graduate Degrees In Medical Physics," Revision of AAPM Report No. 44. AAPM Education and Training of Medical Physicists Committee (2002)
- No. 80 "The Solo Practice of Medical Physics in Radiation Oncology: Report of TG #1 of the AAPM Professional Information and Clinical Relations Committee" (2003)

- No. 81 “Dosimetric Considerations for Patients with Hip Prostheses Undergoing Pelvic Irradiation: Report of the AAPM Radiation Therapy Committee Task Group 63,” Reprinted from *Medical Physics*, Vol. 30, Issue 6 (2003)
- No. 82 “Guidance Document on Delivery, Treatment Planning, and Clinical Implementation of IMRT: Report of the IMRT subcommittee of the AAPM Radiation Therapy Committee,” Reprinted from *Medical Physics*, Vol. 30, Issue 8 (2003)
- No. 83 “Quality Assurance for Computed-Tomography Simulators and the Computed-Tomography-Simulation Process: Report of the AAPM Radiation Therapy Committee Task Group No. 66,” Reprinted from *Medical Physics*, Vol. 30, Issue 10 (2003)
- No. 84 “A Revised AAPM Protocol for Brachytherapy Dose Calculations (Update of AAPM TG 43; Report No. 51),” Report of the Low Energy Interstitial Brachytherapy Subcommittee of the Radiation Therapy Committee, Reprinted from *Medical Physics*, Vol. 31, Issue 3 (2004)
- No. 85 “Tissue Inhomogeneity Corrections for Megavoltage Photon Beams,” AAPM Task Group #65 Radiation Therapy Committee (July 2004)
- No. 86 “Quality Assurance for Clinical Trials: A Primer for Physicists,” Report of the AAPM Subcommittee on Quality Assurance Physics for Cooperative Trials of the Radiation Therapy Committee (October 2004)
- No. 87 “Diode in vivo Dosimetry for Patients Receiving External Beam Radiation Therapy,” AAPM Task Group #62 Radiation Therapy Committee (February 2005)

Further copies of this report and pricing and availability of other AAPM reports and publications may be obtained from:

Medical Physics Publishing
4513 Vernon Blvd.
Madison, WI 53705-4964
Telephone: 1-800-442-5778 or
608-262-4021
Fax: 608-265-2121
Email: mpp@medicalphysics.org
Web site: www.medicalphysics.org